Modeling Seasonal Effects of River Flow on Water Temperatures in an Agriculturally Dominated California River

J. Eli Asarian[1], Crystal Robinson[2]

[1]Riverbend Sciences, Eureka, CA, USA, [2]Quartz Valley Indian Reservation, Fort Jones, CA, USA.

Corresponding author: J. Eli Asarian (eli@riverbendsci.com)

Key Points:

- In this snowmelt and groundwater-influenced river, cool water temperatures lasted longer into summer in high-flow years than low-flow years
- Statistical water temperature model predictions became more accurate when the influence of river flow was allowed to vary seasonally
- These accessible methods can be used to model any river or stream with daily long-term flow and water temperature measurements

Abstract

Low summer river flows can increase vulnerability to warming, impacting coldwater fish. Water managers need tools to quantify the complex linkages between flow and water temperature, yet statistical models often assume a constant relationship between these variables. In California's snowmelt and groundwater-influenced Scott River where agricultural irrigation consumes most summer river flow, flow variation had stronger effects on water temperature in April–July than other months. Using 24 years of daily air temperature and flow data as predictors, we compared multiple statistical methods for modeling daily Scott River water temperatures, including generalized additive models with non-linear interactions between flow and day of the year. Models with seasonally varying flow effects performed better than those assuming a constant relationship between water temperature and flow. Cross-validation root mean squared errors of the selected models were ≤1 °C. We applied the models to several instream flow scenarios currently being considered by stakeholders and regulatory agencies. Relative to historic conditions, the most protective flow scenario would reduce average annual maximum temperature from 25.9 °C to 24.6 °C, reduce average annual degree-days exceedance of 22 °C (a cumulative thermal stress metric) from 107 to 54, and delay the onset of water temperatures greater than 22 °C during some drought years. Withdrawal of river water after 1 June, including for groundwater management purposes, could contribute to additional exceedances of 22 °C. These methods can be applied to model any stream with long-term flow and water temperature measurements, with applications including scenario prediction and infilling data gaps.

Plain Language Summary

Warm water threatens culturally and economically important salmon in Pacific Northwest rivers, including our Scott River study area, causing chronic stress or even mortality. Climate change and agricultural water use have reduced summer river flow in recent decades, intensifying water scarcity. Years with deep mountain snowpack and resulting high groundwater levels extend the high flow season and keep water temperatures cool through the end of July, whereas in drought years the river warms sooner. We used 24 years of river flow and air temperature data to create computer models that simulate water temperatures, provide a tool for assessing the effects of water management. Our models allow the effect of flow on water temperatures to vary by season (i.e., stronger cooling in spring and summer), improving accuracy of the simulated temperatures. We used these models to simulate water temperatures under two alternative flow scenarios being considered in local water management plans. Our simulations indicate that relative to current conditions, the higher flow scenario would reduce the summer's hottest temperatures. Diverting additional water from the river after 1 June could increase the number of days with warm river temperatures that are detrimental to fish. Our model is freely available for public use.

1 Introduction

Water temperature in rivers and streams affects everything from water chemistry and physics to inter-species interactions (Wenger et al., 2011), food webs (Power and Dietrich, 2002), and whole-community metabolism (Bernhardt et al., 2017). Effects on individual species include development (Steel et al., 2012), thermal tolerances (Dahlke et al., 2020), bioenergetics (Gibeau and Palen, 2020), and behavior (Sutton and Soto, 2012).

The net balance of surface and streambed heat fluxes determine stream temperatures. These energy fluxes include shortwave radiation (primarily from the visible light spectrum), longwave radiation (i.e., heat radiated from objects including clouds, land, and vegetation), latent heat (i.e., evaporation), sensible heat (i.e., convection of heat from air to water), conduction of heat between the water and stream bed, and advection (i.e., movement of water) (Caissie, 2006; Moore et al., 2005a; Webb et al., 2008; Dugdale et al., 2017). Humans affect stream temperatures through water diversions (Bartholow, 1991; Dymond J.,1984; Folegot et al., 2018; Gibeau and Palen, 2020; Meier et al. 2003, Null et al.; 2017), discharge of industrial wastewater and sewage (Erickson and Stefan, 2000), reservoir impoundments (Webb and Walling, 1993; Chandesris et al., 2019), removal or enhancement of riparian vegetation (Johnson, 2004; Moore et al. 2005a, Wondzell et al., 2019), and alteration of channel and floodplain morphology (Gu and Li, 2002) including urbanization (Tan and Cherkauer, 2013). Stream temperatures have warmed in recent decades in response to rising air temperatures resulting from anthropogenic greenhouse gas emissions, a trend that is expected to continue (Isaak et al., 2017, 2018; Liu et al., 2020; Wanders et al., 2019).

River flow rates (i.e., discharge) can affect stream temperatures. Higher flows increase a stream's ability to store heat, reducing the temperature increase resulting from an equivalent amount of solar radiation (Brown, 1969; Meier et al., 2003; Sinokrot and Gulliver, 2000). Higher flow rates reduce daily temperature maximums and ranges (Folegot et al., 2018). Summer stream temperatures are typically negatively correlated with flow (Arora et al., 2016; Isaak et al., 2017; Luce et al., 2014; Mayer, 2012; McGrath et al., 2017; Moore, et al. 2005b; Neumann et al, 2003; Webb et al., 2003), with flow affecting daily maximum temperatures more strongly than daily mean temperatures (Asarian et al., 2020; Gu et al., 1998; Gu and Li, 2002). Stream temperature model fit often increases when flow is included as a predictor (Hilderbrand et al., 2014; Piotrowski and Napiorkowski, 2019; Rahmani et al., 2020; Sohrabi et al., 2017; van Vliet et al. 2011; Webb et al., 2003), although not always (Benyahya et al., 2008; Toffolon and Piccolroaz, 2015). Cooling effects of high flows are due to faster downstream transport of cold water (Bartholow, 1991; Dymond J., 1984; Folegot et al., 2018), greater depth and thermal mass which is more resistant to heating (Gu and Li, 2002; Meier et al., 2003; Sinokrot and Gulliver, 2000), and greater accretion of cool groundwater (Kelleher et al., 2012; Mayer, 2012; Isaak et al., 2017).

The relationship between water temperature and flow varies seasonally. The source and flow paths of river water vary seasonally according to precipitation form (i.e., snow and rain)(Siegel and Volk, 2019), groundwater dynamics of hillslope (Hahm et al., 2019) and alluvial (Foglia et al., 2013) aquifers, and irrigation management (i.e., water withdrawals and subsequent return flows back to the river via surface or groundwater)(Tolley et al., 2019). Flow effects on water temperature are also seasonally mediated by variables that affect the amount of solar radiation striking the water, including day length, solar angle (Piotrowski and Napiorkowski, 2019; Yard et al., 2005), cloud cover (Dugdale et al., 2017), wildfire smoke (Asarian et al., 2020; David et al., 2018), and leaf out and leaf fall of deciduous riparian vegetation (Dugdale et al., 2018). Some of these variables follow exactly the same seasonal trajectory each year while others fluctuate among years.

Given stream temperature's importance and vulnerability to human alterations of river flow, water managers need predictive tools. Stream temperature models are often grouped into two categories: process-based and statistical (Caissie, 2006). Process-based (i.e., deterministic) models simulate stream energy budgets using physically based equations representing energy fluxes such as shortwave radiation, longwave radiation, latent heat, sensible heat, conduction and advection (Brown, 1969; Caissie, 2006; Dugdale et al., 2017). Statistical models use empirical relationships between stream temperature and predictor variables, and typically require many fewer variables as data inputs than process-based models do, so are often much simpler to develop (Benyahya et al., 2007; Caissie, 2006; Gallice et al., 2015; Ouellet et al., 2020; Piotrowski and Napiorkowski, 2019). Mohseni et al.'s (1998) non-linear regression of stream temperature and air temperature has been widely replicated (Arismendi et al. 2014; Jones al. 2016) and adapted (Piotrowski and Napiorkowski, 2019; Santiago et al., 2017; Segura et al. 2015; van Vliet et al. 2011). Recent advances in statistical models of stream temperature include spatial stream network models (FitzGerald et al., 2021; Isaak et al., 2017), generalized additive models (GAM) (Arora et al., 2016; Jackson et al., 2018; Laanaya et al., 2017; Siegel and Volk, 2019; Yang and Moyer, 2020), Least Absolute Shrinkage and Selection Operator regression (St-Hilaire et al., 2018), functional data analysis (Boudreault et al., 2019), and machine learning (Rahmani et al., 2020; Zhu et al., 2018, 2020). Daily stream temperatures are highly correlated with adjacent days' temperatures. For measurements such as daily stream temperature that are not independent, it is best to use a model that explicitly includes the correlation structure (Steel et al., 2013). For example, some stream temperature models include a first-order (AR-1) (Benyahya, 2007b; David et al., 2018; Letcher et al., 2016; Jackson et al., 2018; Sohrabi et al., 2017), second-order, periodic (Benyahya et al., 2007a, 2007b, 2008), or moving average autoregressive error structures (Yang and Moyer, 2020).

Process-based models account for the seasonal effects of flow by explicitly modeling energy fluxes, but it is infeasible to include all these individual fluxes in statistical model. However, statistical models can represent the implicit aggregation of these fluxes by allowing the coefficients of hydroclimatic predictors to vary seasonally. One approach is to divide the year into multiple seasons and develop separate models for each (Mohseni et al., 1998, Sohrabi et al., 2017), but this may create abrupt changes at seasonal transitions. Recent approaches that allow smooth variation across seasons are time-varying coefficient models (Li et al., 2014), and GAMs that interact day of the year with predictor variables (Jackson et al., 2018; Siegel and Volk, 2019; Yang and Moyer, 2020).

To test the hypothesis that statistical models with seasonally varying effects of river flow would perform better than models with a constant relationship between stream temperature and flow, we modeled daily stream temperatures in the Scott River of Northern California where low flows and high temperatures are limiting factors for culturally and economically important coldwater fish. We compared multiple statistical approaches that: 1) include all days in a single model rather than dividing the year, 2) use interactions to allow the influence of predictors to vary smoothly by day of the year, 3) allow non-linear relationships, 4) have error structures that include temporal autocorrelation, and 5) are all implemented within the R software environment with simple, publicly accessible code. After model selection and validation which confirmed our hypothesis, we applied our final model to predict daily stream temperatures under flow scenarios being considered by local water managers. Results indicated that stream temperatures under these flow scenarios would be more favorable for coldwater fish than the historic flow scenario. Our accessible modeling approach could be widely replicated in other geographic areas to provide accurate stream temperature predictions to inform river management. Paired with air temperatures from a nearby weather station, our methods can be applied in any river or stream with long-term measurements of flow and stream temperature. Other potential applications include imputing missing measurements for analyses that require continuous temperature time series.

2 Study Area

The Scott River is a tributary of the Klamath River in Siskiyou County, California, USA (Figure 1). The climate is Mediterranean with precipitation occurring primarily in winter and spring as rain at low elevations and snow at higher elevations. The mountainous headwaters are primarily National Forest, with elevations exceeding 2500m (Foglia et al., 2013). The human population lives primarily on private land in the alluvial Scott Valley, where irrigated agriculture is the dominant land use, utilizing groundwater and surface water (Foglia et al., 2018). Other land uses include timber harvest and mining. There are many water diversions but no major dams or reservoirs. The valley aquifer fills during the high flows of winter rainstorms and spring snowmelt-driven runoff. As runoff recedes through the summer, most surface water is diverted for irrigation and river water at the valley outlet becomes increasingly composed of groundwater from valley alluvium. Minimum flows occur in early September before rising due to fall rains (Figure 2). In late summer of drought years, portions of the river have no surface flow (Tolley et al. 2019). Summer and fall river flows have declined in recent decades (Kim and Jain, 2010; Asarian and Walker, 2016) due to a combination of climate change (Drake et al., 2000) and increased withdrawal of groundwater for irrigation, especially since 1977 (Van Kirk and Naman, 2008). Climate change is expected to further reduce summer flows by decreasing snowpack and increasing irrigation demand (Persad et al., 2020). There are ongoing efforts to model interactions between groundwater and surface water (Foglia et al., 2013, 2018; Tolley et al., 2019). Pursuant to California's Sustainable Groundwater Management Act (SGMA), Siskiyou County is developing a groundwater sustainability plan for the valley.

The Scott River has the Klamath Basin's largest population of Endangered Species Act-listed coho salmon (*Oncorhynchus kisutch*) population, despite currently impaired habitat (NMFS, 2014). High water temperatures are stressful to coho salmon, chinook salmon (*Oncorhynchus tshawytscha*) and steelhead (*Oncorhynchus mykiss*) (NCRWQCB, 2005). These fishes' importance to local Native American tribes has led to contention over water management. Government agencies, tribes, and local organizations have studied Scott River stream temperatures for several decades (Asarian et al., 2020; KNF, 2010; Quigley et al., 2001; QVIR, 2016). The river is listed as impaired under the Clean Water Act, and California's North Coast Regional Water Quality Control Board developed Total Maximum Daily Loads (TMDLs) for water temperature and sediment (NCRWQCB, 2005).

Our study site is located at the outlet of Scott Valley, with a drainage area of 1,714 km^2 (Figure 1). Despite simulated total valley-wide streamflow depletion (i.e., decreased streamflow due to groundwater pumping) of approximately 150,000 m^3d^{-1} (60 ft^3/sec) in August (Foglia et al., 2013), the 10 kilometers of river directly upstream of our study site are primarily a gaining reach, receiving groundwater from the alluvial aquifer (Tolley et al., 2019).

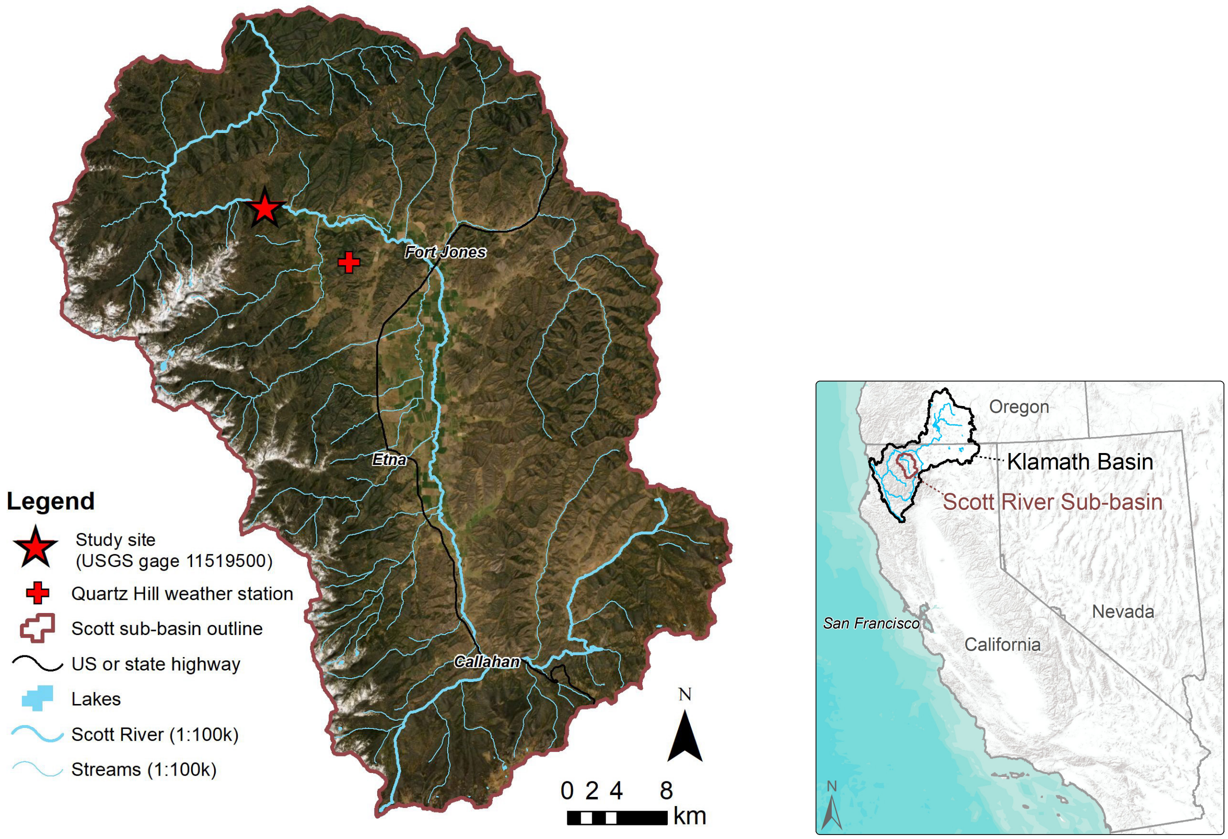

Figure 1. Maps of study site and weather station within the Scott River watershed, the Klamath Basin, and California. Source map credits: Esri, Earthstar Geographics, NOAA, and USGS.

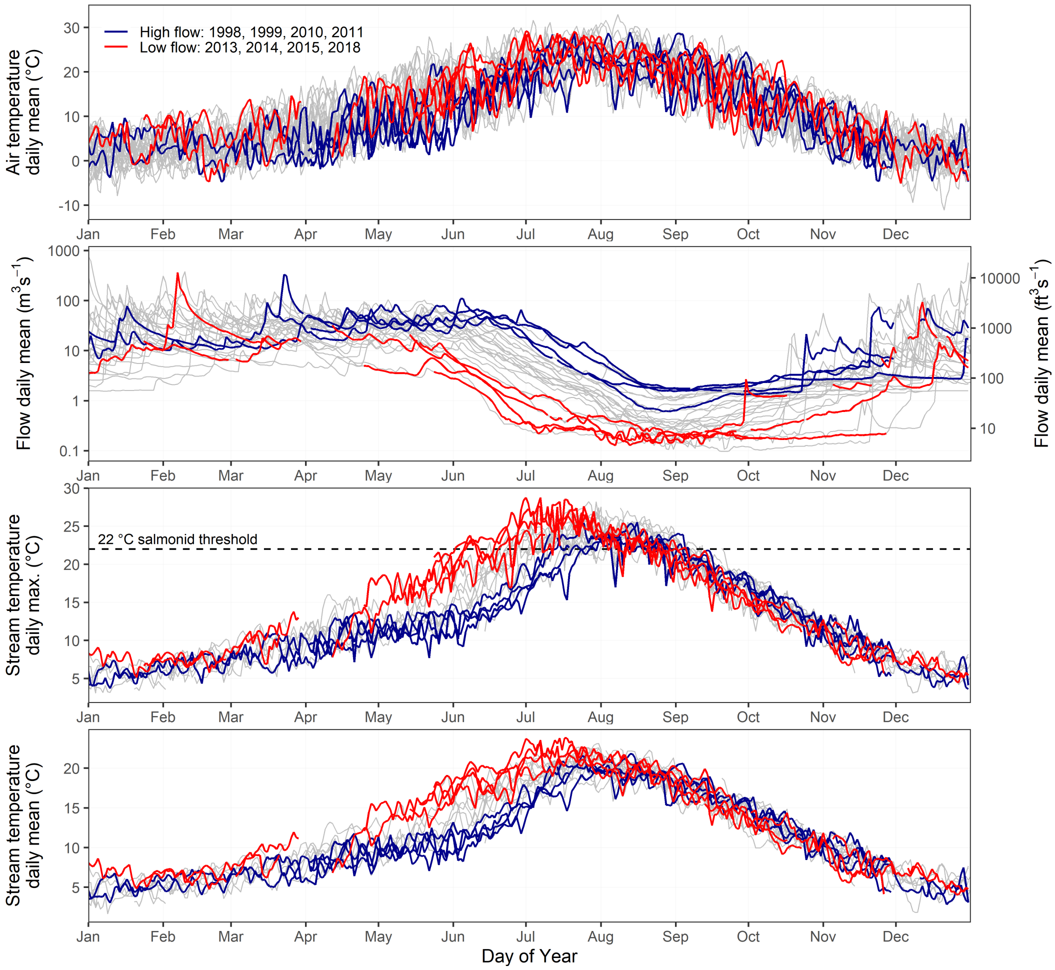

Figure 2. Time series of daily mean air temperature, daily mean flow, daily maximum stream temperature (DMxST), and daily mean stream temperature (DMST) for the years 1995–2020. Colored lines are days in four example high-flow (red) and low-flow years (blue). Gray lines are other years.

3 Methods

3.1 Data sources and data preparation

3.1.1 Water temperature and river flow

Since 2007, the Quartz Valley Indian Reservation (QVIR) Environmental Department has been using YSI (Yellow Springs, Ohio) 6600 multi-parameter datasondes to monitor Scott River water temperatures at the U.S. Geological Survey (USGS) gage 11519500 near the outlet of Scott Valley (QVIR, 2016; Asarian et al., 2020) (Figure 1). Temperature measurements are recorded every 30 minutes with a reported accuracy of ±0.15 °C. We combined QVIR's dataset with additional temperature data collected at the same site by the U.S. Forest Service (USFS) in the years 1995–1998, 2003–2005, 2010–2016, and 2019 (KNF, 2010), and U.S. Bureau of Reclamation (USBR) for the years 1998–2000. Following compilation, we reviewed the data and removed any suspicious values (e.g., when there were calibration issues or probes appear to have been exposed to air). We then calculated daily mean stream temperature (DMST) and daily maximum stream temperature (DMxST). For days when data were available from multiple entities, we averaged values (Text S1).

Daily average streamflow for gage 11519500 were downloaded from the USGS National Water Information System.

3.1.2 Air temperature

Daily mean air temperature data from USFS' Quartz Hill weather station located approximately 8 km southeast of the flow gage (Figure 1) are available as Global Historical Climatology Network - Daily station USR0000CQUA (Menne et al., 2012a, 2012b). We excluded all dates with a quality flag. For days lacking Quartz Hill measurements (0.5% of days with measured stream temperatures and 3.8% of the all days 1995–2020), we infilled missing values by linear regression with nearby weather stations or the gridded PRISM dataset (Daly et al., 2008) (Text S2).

Stream temperatures are correlated with air temperatures at multiple time scales. The optimal number of days to average for regression modeling varies (Webb et al., 2003). In addition to simple averages across varying numbers of days, other approaches include applying exponential weights (Koch and Grünewald, 2010; Piotrowski and Napiorkowski, 2019; Soto, 2016) or including separate terms for air temperatures on the day of interest and preceding days (Siegel and Volk 2019). We tested five categories of air temperatures covariates in our models, where A_i is the mean air temperature on the day *i*, using Equations (1), (2), (3), (4), and (5):

Single-day average A_1:

$$A_1 = A_i \tag{1}$$

Multi-day averages $A_2 \ldots A_7$:

$$A_2 = \frac{(A_i + A_{i-1})}{2}, \ldots , A_7 = \frac{(A_i + A_{i-2} \ldots A_{i-6})}{7} \tag{2}$$

Multi-day weighted averages A_{2w} and A_{3w}, with preceding days discounted by 50% per day:

$$A_{2w} = A_i + \frac{(0.5 * A_{i-1})}{1.5} \text{ and } A_{3w} = \frac{(A_i + 0.5A_{i-1} + 0.25A_{i-2})}{1.75} \tag{3}$$

Lagged averages A_{L3} and A_{L5}:

$$A_{L3} = \frac{(A_{i-1} + A_{i-2} + A_{i-3})}{3} \text{ and } A_{L5} = \frac{(A_{i-1} + A_{i-2} + A_{i-3} + A_{i-4} + A_{i-5})}{5} \tag{4}$$

Differences between lagged average and day *i*:

$$A_{\Delta 3} = (A_i - A_{L3}) \text{ and } A_{\Delta 5} = (A_i - A_{L5}) \tag{5}$$

To improve numerical stability, we standardized each air temperature and flow predictor variable by centering (i.e., subtracting the mean) and scaling (i.e., dividing by the standard deviation).

3.2 Model development and calibration

We developed statistical models to predict DMxST and DMST using river flow and air temperature as predictors (Table 1). We tested three classes of models: non-linear logistic regression, harmonic regression, and generalized additive models (GAM). Models were developed in R version 4.02 (R Core Team 2020).

3.2.1 Generalized additive models (GAMs)

We focused our stream temperature modeling on GAMs because they offer powerful flexibility including non-linear smoothers (Pedersen et al., 2019; van Rij et al., 2019). We used the bam function in the mgcv R package version 1.8-31 (Wood, 2017) to develop GAM models, fit using fast restricted maximum likelihood (fREML). GAM model terms can be either linear coefficients or non-linear functions (Wood, 2017; Pedersen et al., 2019). The non-linear functions are smooth curves with the amount of wiggliness automatically determined by a smoothing penalty. We used cyclic cubic regression splines ("cc") as the smoother for day of the year D and thin plate regression splines ("tp") as smoothers for other covariates. To avoid overfitting (Siegel and Volk, 2019) we limited smoothers for most variables to a maximum of 3 knots, except D which was allowed up to 5 knots.

We compared GAMs that allow the relationships between covariates and the response variable to vary seasonally to GAMs where those relationships are seasonally constant. Our GAM models represented interactions between variables as either partially non-linear or fully non-linear. For a partially non-linear interaction, the linear slope of one variable (e.g., flow) changed as a smooth non-linear function of another variable (i.e., D), an approach used by Jackson et al. (2018) and Siegel and Volk (2019) and specified in mgcv using the "by" option. Fully non-linear relationships between two or more variables were specified as tensor product smooths in mgcv using the syntax "te()" (Wood, 2017). If main effects were included as separate terms, then we used "ti()"to specify a tensor product interaction (Wood, 2017).

All our GAM models included a random effect for year and all but one ("GAM11," Section 4.2) included an AR-1 autocorrelation error structure. The bam function cannot automatically derive the AR-1 coefficient (rho), so it must be manually assigned. Following Baayen et al. (2018) and van Rij et al. (2019, 2020), we initially fit each model without an autocorrelation term, and then re-ran the model with an autocorrelation term, assigning a rho value based on the lag 1 autocorrelation from the residuals of the initial model. Baayen et al. (2018) and van Rij et al. (2019) advise testing several rho values using model-comparison procedures, which in our case always confirmed the initial values were optimal.

3.2.2 Harmonic regression

As an alternative to compare to GAMs, we use harmonic regression (also known as trigonometric or periodic regression) (Cox, 2006) with paired sine and cosine interaction terms that allow the slope of covariates to vary as a smooth cycle over the course of the year (Bodeker et al., 1998). For daily periodicity, we multiplied day of the year D by $2\pi/365$ (Helsel et al., 2020). We developed these models using the lme function in the nlme R package version 3.1-148 (Pinheiro et al., 2020) with an AR-1 autocorrelation term and a random intercept for year, fit using maximum likelihood (ML). Harmonic regression of stream temperature is common (Kothandaraman, 1971; Johnson et al., 2020), but we are not aware of previous applications of harmonic interactions between D and other covariates for stream temperatures.

3.2.3 Non-linear logistic regression

Since Mohseni et al.'s (1998) non-linear logistic regression of air temperature and stream temperature has been so widely applied, we use it as a benchmark to compare our other model to. Many streams, including the Scott River (Manhard et al., 2018), exhibit hysteresis in which the relationship between stream temperature and air temperature differs between spring and fall (Mohseni et al., 1998). Following Jones et al.'s (2016) code using R's optim function, we modeled the ascending (weeks 1–30) and descending (weeks 31–52) limbs separately, fitting models using weekly averages and then apply them to daily data. These models do not include flow, autocorrelation, or random effects. We used 7-day average air temperatures to match the original method.

3.3 Model selection and validation

We compared alternative model configurations (which variables and interactions are included, which are assigned random effects, etc.) to select a final model (Table 1). Initial exploration indicated that A_{2w} (2-day weighted air temperature) provided better model fits than other air temperature variables, so we used A_{2w} for most of our models. After final model selection, we developed a separate set of models to assess the sensitivity of model fits to using different air temperature variables (Figure S1). Rather than slavishly follow a pre-specified procedure such as forward-selection or backward selection, we took a more holistic approach to model selection. We selected a final model after considering multiple models using a variety of methods including Akaike information criterion (AIC), fREML (fast restricted maximum likelihood) scores for GAMs, goodness of fit metrics (root mean squared error [RMSE] and coefficient of termination [R^2]), and review of residual plots and auto correlation function plots. Concurvity, the non-linear equivalent of collinearity, is a potential concern for GAMs such as ours that contain smooths for time along with other time-varying covariates (Amodio et al., 2014; Wood, 2017), so we evaluated each GAM's concurvity using mgcv's concurvity function.

Prior to modeling, we randomly selected and excluded all data from 4 (17%) of the 24 years. These data were not used in model selection but instead were retained for out-of-sample validation.

We validated models using two methods. First, we used leave-one-year-out (LOYO) cross-validation, a version of k-fold variation in which we withhold a year, re-fit the model using the

19 remaining years, compare predictions for the withheld year against the measured data using goodness of fit metrics (RMSE and R^2), and then repeat the same process for each year. Second, for out-of-sample validation, we compared model predictions (calibrated with 20 years of data) against data from the four removed years using goodness of fit metrics (RMSE and R^2).

3.5 Model application to hydroclimatic and flow management scenarios

To assess the seasonal response of stream temperatures to variation in flow and air temperatures, we applied our selected GAM models to a group of 15 "quantile air temperature" scenarios representing combinations of 3 air temperature inputs and 5 flow inputs (Table 2, Figure 3). All three air temperature inputs were derived using non-parametric quantile regression (Cade and Noon, 2003; Muggeo et al., 2013) to calculate the air temperature associated with three quantiles (0.05, 0.50, and 0.95, equivalent to 5%, 50%, 95% exceedance probabilities) for each day of the year (Figure 3a), using the quantregGrowth R package (Muggeo et al., 2013), with options described in Text S3. For air temperature, the 0.50 quantile represented typical conditions, the 0.05 quantile represented hottest conditions, and the 0.95 quantile represented coolest conditions. Three of the five flow inputs were based on quantiles (0.05, 0.50, and 0.95) derived using similar methods as the air temperature inputs, with the 0.50 quantile representing typical conditions, the 0.05 quantile representing very low flow conditions, and the 0.95 quantile representing high flow conditions (Figure 3b). The remaining two of the five flow inputs are based on the USFS water right and California Department of Fish and Wildlife (CDFW) Interim Instream Flow Criteria. The USFS first-priority Scheduled D water right varies by month and day, from a high of 200 ft^3/sec (5.67 m^3/sec) in November through March to a low of 30 ft^3/sec (0.85 m^3/sec) in August and September (Superior Court of Siskiyou County, 1980) (Figure 3b). The CDFW criteria vary by month and day, from a minimum of 62 ft^3/sec (1.75 m^3/sec) in September to a high of 362 ft^3/sec (10.3 m^3/sec) in February (CDFW, 2017) (Figure 3b). The CDFW and USFS flows do not follow a particular flow quantile through the entire year, but instead are extreme drought conditions in May (0.05 quantile) and high flows in August and September (0.50 to 0.95 quantile).

To assess the realistic timing and magnitude of modeled exceedances of stream temperature thresholds, we also applied our selected GAM model to predict stream temperatures in a group of "observed air temperature" scenarios that pair the observed daily air temperature time series for 1995-2020 with eight flow conditions: observed USGS flows in addition to the five flows used in the "quantile air temperature" scenarios (low, typical, high, USFS, and CDFW) as well as two additional scenarios in which the CDFW and USFS flows are used as minimums that are supplanted by observed USGS flows on dates when the observed flows are higher (Table 2). We expect that using observed air temperatures instead of quantile air temperatures provides more realistic real-world predictions because air temperatures fluctuate erratically from day to day (Figure 2), instead of staying near the same quantile like flow does during the seasonal flow recession each year from May through September.

We summarized the results of each "observed air temperature" scenario by calculating: 1) annual maximum temperature, 2) first and last day each year in which water temperatures exceed 22 °C, and 3) the annual degree days exceedance of 22 °C, calculated by subtracting 22 from all DMxST and summing all positive values by year. We chose 22 °C as an indicator of biological effects on juvenile salmonids that rear in the mainstem Scott River or outmigrate downstream using the river as a migratory corridor. Given the potential for local genetic adaptation to thermal regimes (Zillig et al., 2021), we prioritized studies near the Scott River in selecting thresholds. When the Klamath River exceeds 22–23 °C, juvenile salmonids move to tributary confluences (Sutton et al., 2007; Sutton and Soto, 2012; Brewitt and Danner, 2014). Similar behavior was observed in the Shasta River (Nichols et al., 2014) and 22 °C was also used by McGrath et al. (2017). The 22 °C threshold is not fully protective for coho salmon (Text S4) but we chose it because our study site is a mainstem river where temperatures are expected to be higher than a cool tributary.

Table 1. Comparison of model training statistics.

		Daily maximum stream temperature (DMxST)						Daily mean stream temperature (DMST)					
Model Name	**Predictor variables**	**fREML**	**AIC**	**AR1**	**edf**	**RMSE**	**R^2**	**fREML**	**AIC**	**AR1**	**edf**	**RMSE**	**R^2**
GAM1: tensor Q-A_{2w}-D	te(Q, A_{2w}, D)	5004	9901	0.587	46.5	0.86	0.982	3354	6607	0.747	46.5	0.77	0.979
GAM2: tensors Q-D & A_{2w}-D	s(A_{2w}) + ti(A_{2w}, D) + te(Q, D)	5036	9973	0.603	36.4	0.88	0.981	3364	6639	0.769	35.6	0.80	0.978
GAM3: tensor Q-D & vary A_{2w}	s(D, by = A_{2w}) + te(Q, D)	5039	9978	0.580	39.3	0.86	0.982	3373	6649	0.742	39.1	0.75	0.980
GAM4: tensors Q-D & A_{2w}-Q (final)	s(D, by = A_{2w}) + ti(A_{2w}, Q) + te(Q, D)	5053	10022	0.603	36.3	0.89	0.981	3401	6729	0.763	35.4	0.80	0.978
GAM5: tensors Q-D & A_{2w}-Qv2	s(A_{2w}) + ti(A_{2w}, Q) + te(Q, D)	5095	10116	0.608	34.1	0.90	0.98	3452	6840	0.764	33.2	0.82	0.977
GAM6: tensor Q-D no vary A_{2w}	s(A_{2w}) + te(Q, D)	5105	10139	0.611	30.4	0.90	0.98	3466	6873	0.77	28.6	0.83	0.976
GAM7: varying Q & A_{2w}	s(D, by = A_{2w}) + s(D, by = Q) + s(D)	5160	10254	0.659	28.2	0.96	0.978	3464	6871	0.804	27.5	0.88	0.973
GAM8: A_{2w} *no varying*	s(A_{2w}) + s(Q) + s(D)	5448	10855	0.773	23.1	1.35	0.956	3626	7208	0.834	23.8	1.08	0.96
GAM9: A_{2w} *no Q or varying*	s(A_{2w}) + s(D)	5525	11010	0.846	22.3	1.70	0.931	3749	7459	0.875	21.6	1.30	0.941
GAM10: A_7 only with AR1	s(A_7)	6606	13186	0.886	21.3	2.75	0.817	5044	10062	0.905	21.2	2.29	0.819
GAM11: A_7 only no AR1	s(A_7)	10441	20823	N/A	23.2	2.21	0.882	9330	18602	N/A	23.1	1.74	0.895
Harmonic12: varying Q & A_{2w}	A_{2w} + A_{2w}:sin(Dn) + A_{2w}:cos(Dn) + Q + Q:sin(Dn) + Q:cos(Dn) + cos(Dn) + sin(Dn)	N/A	10368	0.73	N/A	1.04	0.969	N/A	6810	0.859	N/A	0.94	0.964
Logistic13: Mohseni	Logistic regression with A_7	N/A	N/A	N/A	N/A	2.34	0.868	N/A	N/A	N/A	N/A	1.84	0.883

Note: GAM models are sorted by fREML score for DMxST. Except 'GAM11 A_7 only no AR1', all GAM and LMM models also include an AR1 autocorrelation structure and a random effect of year. For models with italicized names, validation statistics are provided in Figures 4 (DMxST) and S5 (DMST). D = day of year from 1 (1 January) to 366 (31 December in leap year), Q = daily mean flow in units of m^3/s, see Section 3.1.12 for key to 'A' air temperature variables, 's()' is a non-linear function, 's(D, by =)' is a linear interaction that varies smoothly by D, 'te()' is a fully non-linear tensor product smooth of two or three variables, 'ti()' is a tensor product interaction, ':' is linear interaction, n = 2π/365, fREML = fast restricted maximum likelihood score, AIC = Akaike information criterion, AR1 = autocorrelation coefficient, edf = effective degrees of freedom, RMSE = root mean squared error, and R^2 = coefficient of determination.

Table 2. Matrix showing the 23 stream temperature model scenarios representing combinations of air temperature and flow inputs, and organized into two scenario groups. The 15 scenarios in Group 1 use "quantile air temperature" inputs and 8 scenarios in Group 2 use "observed air temperature" inputs.

Air temperature inputs	**Flow inputs**							
	Lowest (0.05 quantile)	**Typical** (0.50 quantile)	**Highest** (0.95 quantile)	**USFS exact**	**CDFW exact**	**USFS as minimum**	**CDFW as minimum**	**Observed**
Hottest (0.95 quantile)	Group 1	Group 1	Group 1	Group 1	Group 1			
Typical (0.50 quantile)	Group 1	Group 1	Group 1	Group 1	Group 1			
Coolest (0.05 quantile)	Group 1	Group 1	Group 1	Group 1	Group 1			
Observed	Group 2	Group 2	Group 2	Group 2	Group 2	Group 2	Group 2	Group 2

Note: USFS = USFS Schedule D first-priority water right (Superior Court of Siskiyou County, 1980), and CDFW = CDFW Interim Instream Flow Criteria (CDFW, 2017). See text for explanation of quantiles and flow minimums.

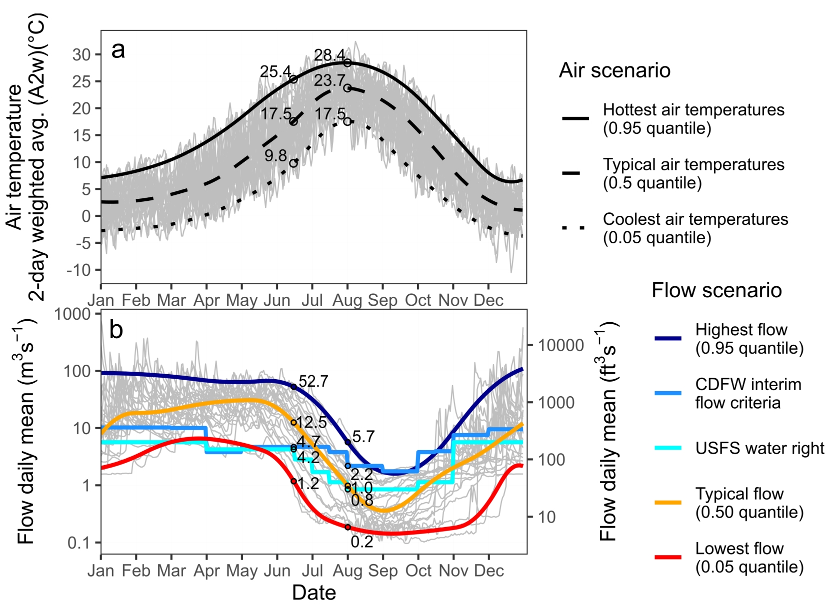

Figure 3. Inputs to Group 1 scenarios representing 15 combinations of (a) three air temperature inputs and (b) five flows inputs that vary by day. Observed values for 1995–2020 are shown as gray lines in both panels. Data values are labeled for 15 June and 1 August.

4 Results

4.1 Measured water temperature, air temperature, and flow

From May–July, measured water temperatures were highly variable among years (Figure 2). For those months, the highest-flow years had DMxST averaging 6.8 °C cooler than during lowest-flow years, while DMST averaged 5.3 °C cooler. In contrast, from August through October inter-annual differences in water temperature much less pronounced. Annual maximum water temperatures occurred earlier in the season in low-flow years (i.e., early/mid-July) than in high-flow years (i.e., late July or early August). These observations inspired us to develop seasonally varying models.

4.2 Model selection and validation

The sensitivity analysis of model training statistics for models using various air temperature metrics indicated similar performance for most of the metrics, except the longest multi-day air temperature averages which had higher RMSE (Figure S1). For DMxST, RMSE ranged from 0.88–0.90 °C for all air temperature metrics except the 3-day to 7-day averages which were 0.96–1.15 °C (Figure S1). For DMST, RMSE ranged from 0.79–0.82 °C for all air temperature metrics except the 4-day to 7-day averages which were 0.85–0.98 °C and the single-day average (0.87 °C) (Figure S1). Given the excellent performance of the 2-day weighted air temperature (A_{2w}) in predicting both DMxST and DMST (Figure S1), we use A_{2w} for all models except Logistic13 and the two GAM models that mimic it (Table 1).

Validation and training statistics indicate a wide range of performance (Table 1, Figure 4), with the tensor models (i.e., GAM1, GAM2, GAM3, GAM4, GAM5, GAM6) performing best while those models that used only air temperature (e.g., Logistic13 and its GAM equivalent GAM11) performed the worst.

GAM4, chosen as our selected model for reasons discussed in Section 5.1, had a cross-validated RMSE of 1.01 °C for DMxST (Figure 4) and 0.93 °C for DMST (Figure S5), with similar values for out-of-sample validation. Similar to the measured data (Figure 2), in the May–July period the selected model predicts cool water temperatures during high-flow years and warm water temperatures during low-flow years (Figure S2). The effects plot for the selected models show that stream temperatures are relatively insensitive to flow from 1 December to 1 March, but that flow exerts a strong cooling influence from 1 April to 1 August (Figure 5, Figure S7). The complete time series of measured and modeled water temperature data for all years is available as Figure S3 and S4 for DMxST and DMST, respectively.

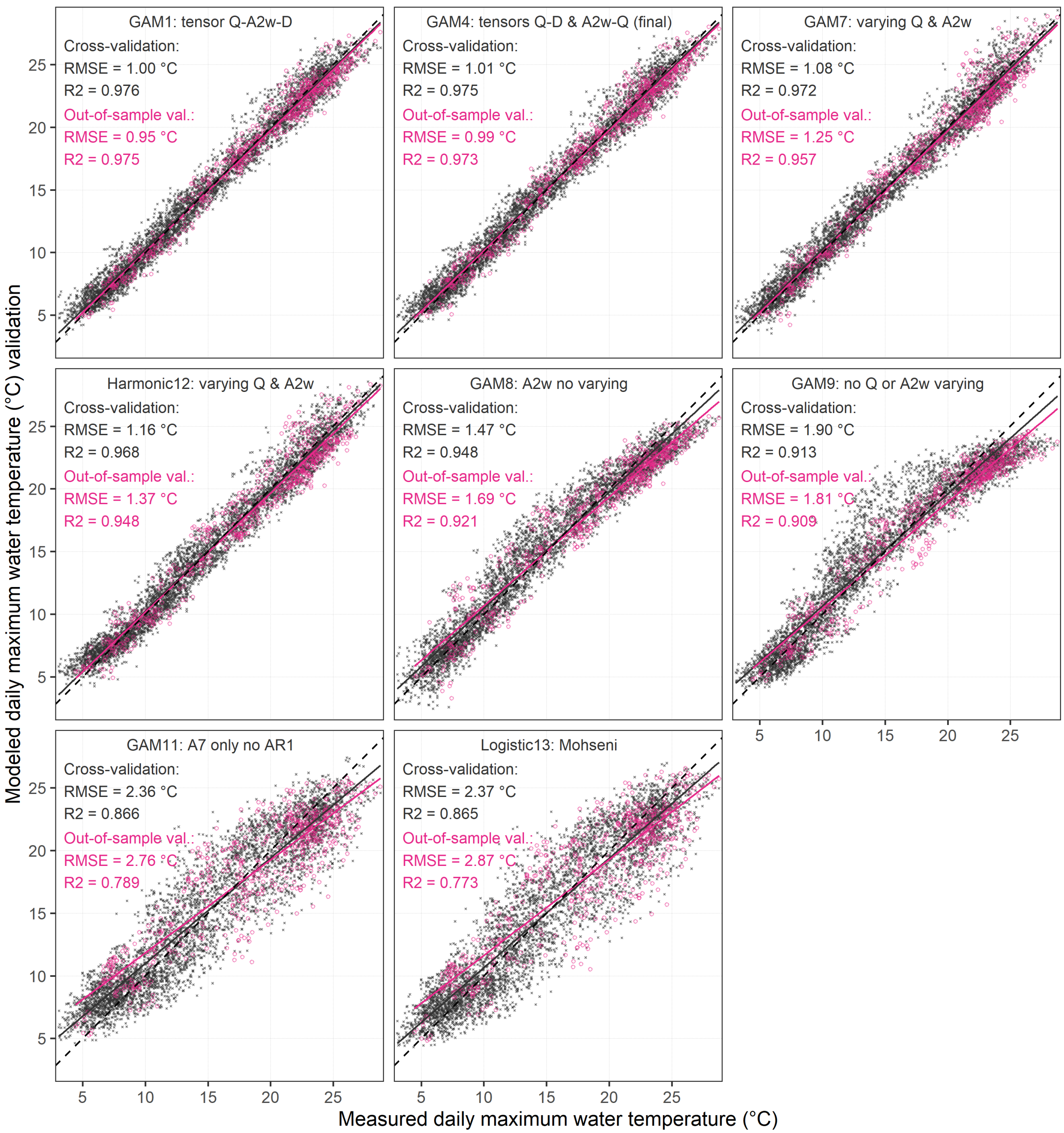

Figure 4. Comparison of measured DMxST to LOYO cross-validation predictions and out of sample validation predictions for 1995–2020. Solid lines are linear regression and dotted lines are the 1:1 (Y=X) lines.

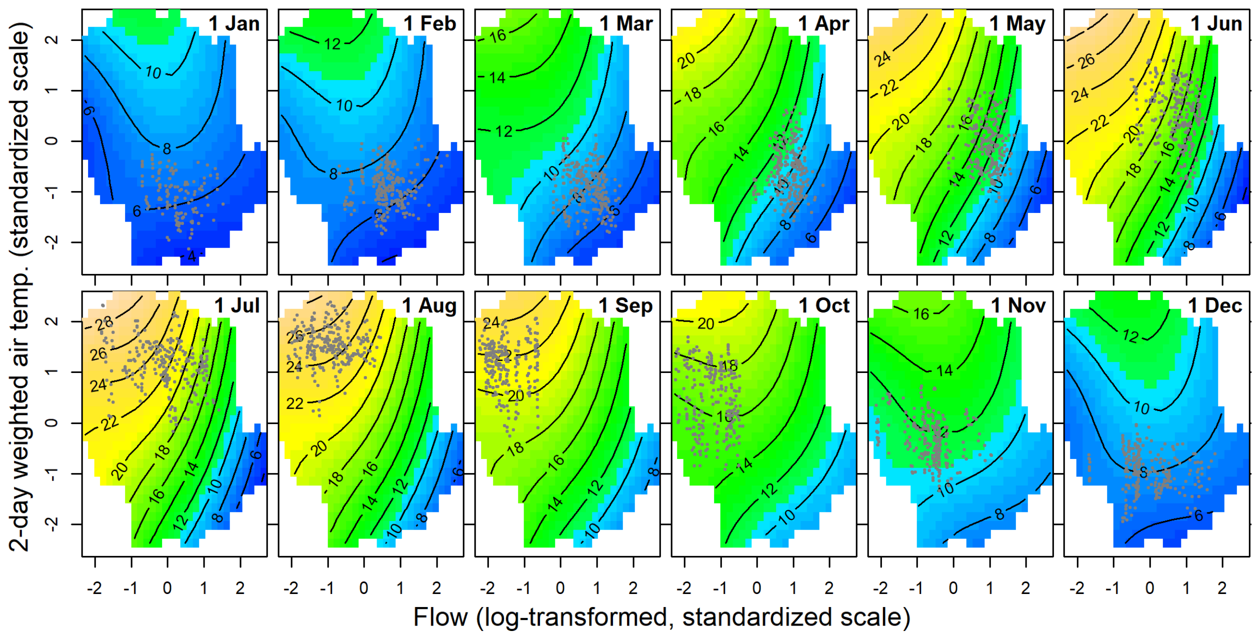

Figure 5. Effects plot showing predictions from selected model "GAM4: tensors Q-D & A2w-Q" that uses 2-day weighted air temperature (A_{2w}), flow (Q), and day of year (D) as predictors. Colors show predicted DMxST as function of Q and A_{2w}, with DMxST labeled contour lines spaced 2 °C apart. Panels represent the first day of each month. Gray dots show position of calibration points within 5 days of first of each month.

4.3 Model application to hydroclimatic and flow management scenarios

The "quantile air temperature" model scenarios show that flow and air temperature both had strong effects on water temperature (Figure 6). The cooling effect of high flow followed a seasonal pattern, rising in March to reach a peak on 15 June (up to 9.5 °C for DMxST and 6.2 °C for DMST), then diminishing to near zero by early September (Figure 6). Cooling effects of high flows were stronger when air temperatures were high than when air temperatures were low (e.g., 15 June difference in DMxST between highest-flow and lowest-flow scenarios is 9.5 °C with the hottest air temperatures and 8.0 °C with the coolest air temperatures). With less solar radiation (due to shorter days and lower solar angle) and lower air temperatures than earlier months, DMxST is almost always less than 22 °C by early September regardless of flow (gray lines in top panels of Figure 6). Consistent with the measured data (Figure 2), modeled annual maximum water temperatures occurred later in the season in high-flow years (i.e., late July or early August) than in low-flow years (i.e., early/mid-July) (Figure 6).

In the "observed air temperature" scenarios, we modeled DMxST pairing the observed air temperature time series for 1995–2020 with eight flow scenarios (Table 2, Figures 7 and S8). These scenarios provide an indication of the range (e.g., due to air temperatures) in daily water temperature associated with each flow scenario. Compared to the lowest flow scenario (0.05 quantile), the highest flow scenario (0.95 quantile) has annual maximum temperatures that are 3.7 °C cooler (Figure 7a) and temperatures first reach 22 °C 51 days later (Figure 7c); in contrast, there is only a 2-day difference in the last day of the year that has temperatures >22 °C (Figure 7d). The scenario with observed flows has the most interannual variation in the annual maximum temperature (Figure 7a) and timing of exceedances of 22 °C (Figure 7c,d), because it includes very low flows as well as very high flows. Water temperatures reach 22 °C 17 days earlier with the exact USFS flows than with observed flows (Figure 7c) because the USFS flows are much lower than average observed flows in May and June. In contrast, in the scenario in which USFS flows are treated as minimums (supplanted by observed flows on days when observed flows are higher), temperatures reach 22 °C on the same day as the observed flow scenario (Figure 7d). Due to high July and August flows in the CDFW scenarios, annual maximum water temperatures are 1.1–1.3 °C cooler in the CDFW scenarios than the observed flow scenario (Figure 7a). Relative to the observed flow scenario, the date that the CDFW as minimum scenario first reaches 22 °C is only 3 days later average (2 July vs. 30 June), but the number of years with exceedances prior to June 20 are reduced from 6 to 2 (Figure 7c) because the CDFW flows are higher in observed flows in drought years. Patterns of inter-scenario differences in annual degree-days exceedance of 22 °C (Figure 7b) are very similar to those of annual maximum temperature (Figure 7a). While the CDFW flows and USFS flows are both predicted to improve (i.e., cool) summer temperatures relative to current conditions, these improvements would be greater with the higher CDFW flows.

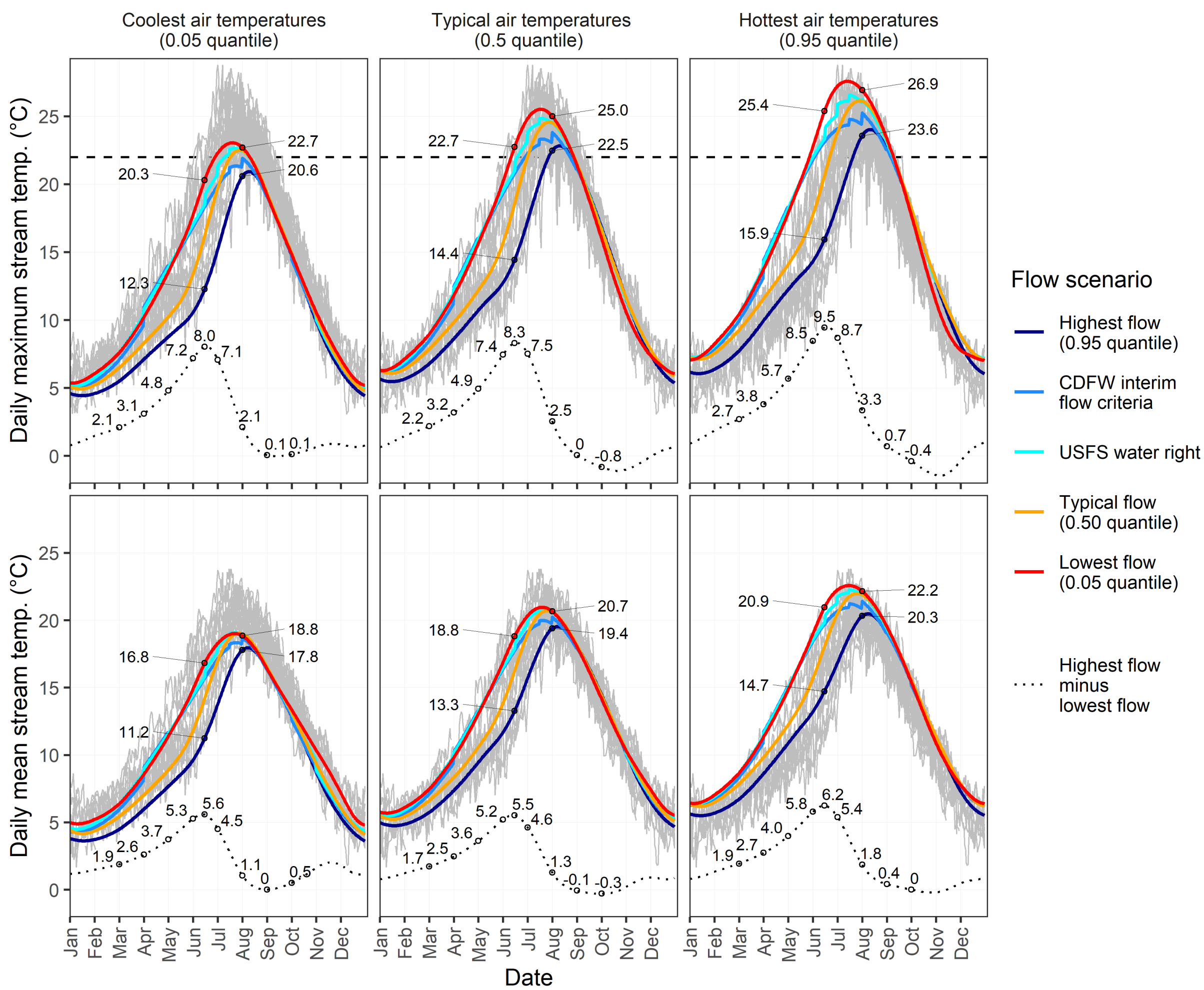

Figure 6. Predicted maximum and mean water temperatures under the 15 “quantile air temperature” scenarios representing combinations of 3 air temperature inputs (arranged in columns) and flow inputs (shown by color). Observed values for 1995–2020 are shown as gray lines. Selected data values are labeled on 15 June and the first day of the months March–October. Horizontal line at 22 °C DMxST is salmonid temperature threshold.

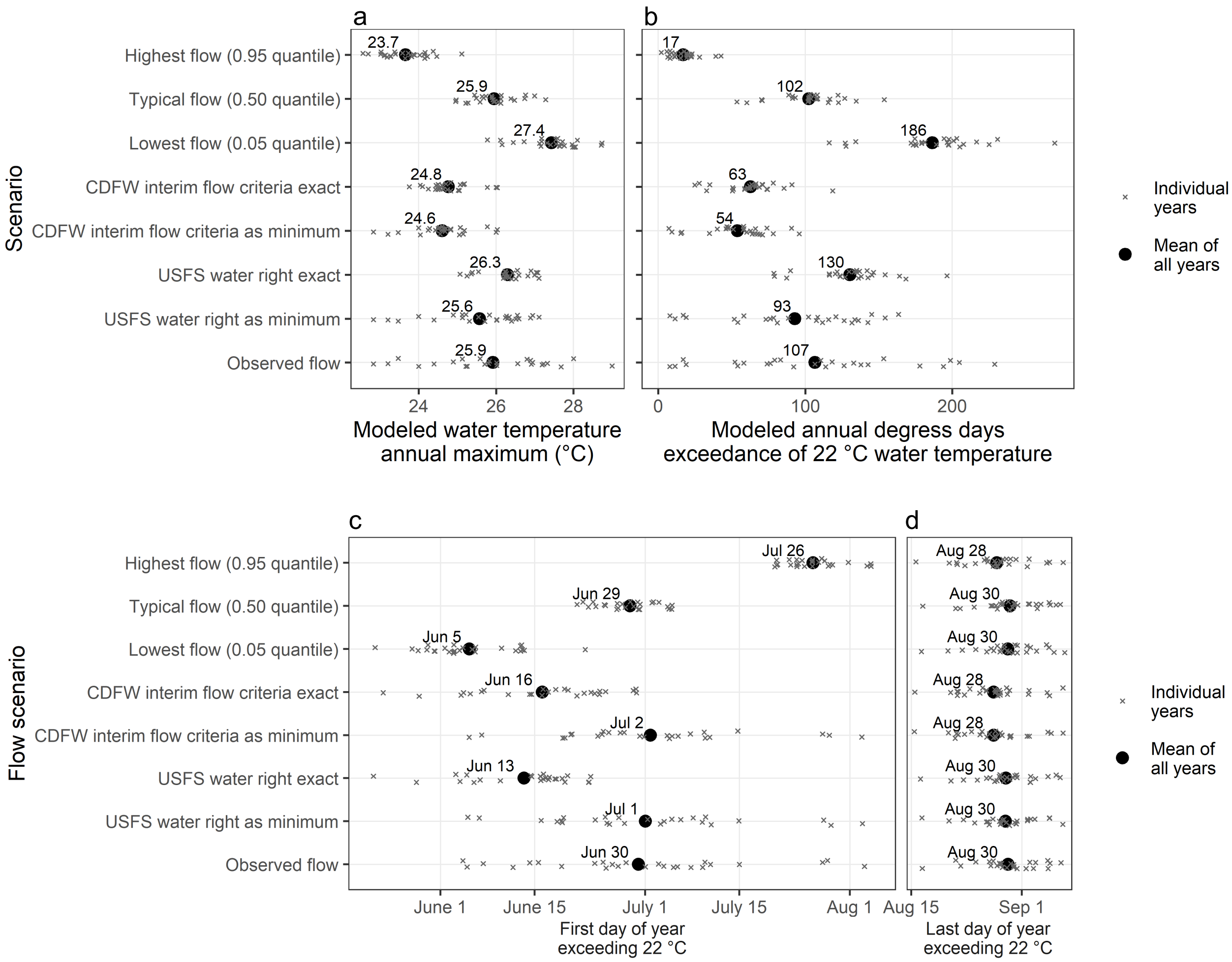

Figure 7. (a) Annual maximum stream temperature, (b) annual degree-days exceeding 22 °C, and (c) first day and (d) last day each year when DMxST exceeds 22 °C predicted using a statistical model pairing observed air temperatures for 1995–2020 with the same eight flow conditions shown in Figure S8. Points for individual years are offset slightly for clarity. Data labels are the mean of all years.

5 Discussion

Consistent with our hypothesis, models with seasonally varying effects of flow outperformed models with a constant relationship between stream temperature and flow. High flows have a strong cooling effect on stream temperatures in April–July, but less influence during other months. The flexibility of GAMs, including non-linear and seasonally varying relationships between stream temperature and flow, produced more accurate predictions than harmonic regression models. Logistic regression of stream temperature with air temperature, based Mohseni et al.'s (1998) popular method, performed particularly poorly in comparison to the GAMs because it did not include flow as a predictor. Our results confirm previous findings that summer stream temperatures are negatively correlated with flow (Arora et al., 2016; Isaak et al., 2017; Luce et al., 2014; Neumann et al, 2003), and that flow more strongly affects DMxST than DMST (Asarian et al., 2020; Gu et al., 1998; Gu and Li, 2002).

5.1 Model selection and the importance of seasonally varying and non-linear relationships

After considering 13 models, we selected the GAM model with a two-day weighted air temperature (A_{2w}) whose slope varies by day of the year (D), a tensor product smooth of flow and day of the year (Q-D), and an A_{2w}-Q tensor product interaction (Table 1, Figure 4). We chose this model (GAM4 "tensors Q-D & A_{2w}-Q") based on a combination of model fit (low RMSE, high R^2, and low fREML score) and fewer effective degrees of freedom (edf) than other models with similar fit. This structure allowed modeled stream temperatures to respond flexibly to varying conditions in all three variables (D, A_{2w}, and Q). Although the three-way tensor GAM1 "tensor Q-D-A_{2w}" had the lowest fREML score, making it an appealing choice, it also had the highest edf, increasing the risk of being overfit. Indeed, when we experimented with applying GAM1 to model scenarios (not shown), the coolest air temperature scenarios (0.05 quantile) had mid-July temperatures that were higher in the typical flow (0.50 quantile) than either the lowest flow (0.05 quantile) or highest flow (0.95 quantile) scenario, which seemed implausible.

Comparing the relative performance of models with different smoothers and interactions provides insight into which are most important (Table 1, Figure 4, Figure S5). All models lacking seasonally varying flow effects (i.e., GAM8, GAM9, GAM10, GAM11, and Logistic13) performed worse than any model with seasonally varying flow effects, highlighting the importance of this feature. Modeled temperatures were biased high in April–June in models without seasonally varying flow effects, an issue that is diminished but still present in the Harmonic12 model that represents seasonal effects as perfectly symmetrical sine waves, and completely absent in the models that represents seasonal effects as flexible GAM smoothers (Figure S6). Models with tensors (i.e., GAM1, GAM2, GAM3, GAM4, GAM5, GAM6) had better fit than models with seasonally varying but linear relationships (e.g., GAM7), though the difference was not as great as the difference between seasonally constant models and seasonally varying models. For example, relative to the GAM7 model which is seasonally varying but linear, the GAM8 model with non-linear but seasonally constant relationships had a RMSE 0.4 C° lower (0.96 °C vs. 1.35 °C) for DMxST and 0.2 C° lower (0.88 °C vs. 1.08 °C) for DMST (Table 1). The selected model, GAM4, which has a fully non-linear tensor product smooth of D and Q, and a tensor product interaction of A_{2w} and Q, has improved (relative to GAM8) RMSE of 0.89 °C for DMxST and 0.80 °C DMST and improved rREML scores (Table 1). In addition, the results for GAM3 (seasonally varying A_{2w} and Q-D tensor product smooth) and GAM5 (A_{2w}-D tensor product interaction and Q-D tensor product smooth), suggests that most of the improvement between GAM7 and GAM4 comes from the Q-D tensor product smooth rather than from the D-varying A_{2w} or Q-A_{2w} tensor product interaction (Table 1).

The GAMs work well because they are able to represent the non-linear relationships and interactions between predictor variables present in our dataset. Heeding guidance from previous researchers we prevented overfitting by limiting the number of knots in the tensors (Jackson et al., 2018; Siegel and Volk, 2019). Our flexible approach takes maximal advantage of our multi-decade daily calibration dataset featuring a range of environmental conditions (i.e., hot and cool air temperatures and high and low flows) over the 4696 days. Our validation results suggest that we have enough data to support our rather complex selected model GAM4. Future researchers modeling temperatures at other sites may not have as much data, so should exercise caution and may want to use the simpler GAM7 model.

5.3 Snow and groundwater mediate the effects of river flow on water temperature

Flow magnitude and seasonality at our study site is driven by a mix of valley groundwater dynamics and snowmelt-driven mountain runoff (Foglia et al., 2013; Van Kirk and Naman, 2008). Groundwater contributes to the relationship between flow and stream temperature at our study site, as it does in many other rivers (Briggs et al., 2018; Kelleher et al., 2012; Mayer, 2012; Nichols et al., 2014; Isaak et al., 2017). Thermal infrared imagery, field measurements (NCRWQCB, 2005), and a groundwater model (Tolley et al., 2019) all confirm that substantial groundwater is forced into the Scott River where the valley constricts upstream of our site, a common phenomenon at the outlet of alluvial valleys (Stanford and Ward, 1992). Process-based model scenarios predicted a doubling of groundwater-derived flow would cool peak summer Scott River temperatures by 2 °C, and a 50% reduction of groundwater-derived flow would warm temperatures by 2 °C (NCRWQCB, 2005).

The timing and magnitude of flow-induced cooling indicated by our models are similar to other snowmelt-dominated rivers. A process-based model of a Sierra Nevada river indicated early summer stream temperatures up to 16 °C cooler in an extreme wet year relative to a dry year (Null et al., 2013). Relative to a statistical model with only air temperature, including flow as a predictor improved stream temperature predictions in April through August in Idaho streams (Sohrabi et al. 2017). Most studies predicting climate change effects do not parse the separate contributions of hydrology and air temperature on stream temperature, but in snow-dominated areas of the western North America, predictions of disproportionate stream temperature warming expected in the summer and/or spring are nearly ubiquitous and attributed to earlier runoff timing from declining snowpack (Caldwell et al., 2013; Crozier et al., 2020; Ficklin et al., 2014; Lee et al., 2020; Leach and Moore, 2019; Luo et al., 2013; Null et al., 2013).

5.4 Biological implications

The prolonged snowmelt-driven flow recession in high-flow years keeps Scott River temperatures cooler longer into the summer than in low-flow years, extending the period when cool water habitat is available for fish (i.e., temperatures less than 22 °C)(Figure 7). These cooler water temperatures give juvenile salmonids additional time to migrate downstream and reduce overall thermal stress for fish that rear in the Scott River through the entire summer. Mean diel range in June–August exceeds 5 °C, providing hours every day when temperatures are less than 22 °C even if DMxST exceeds 22 °C. Salmonids can potentially persist by using thermal refugia where cool tributaries, groundwater, or hyporheic flow enters the river during the hotter parts of the day and then moving into the mainstem to feed when temperatures are cooler (Sutton et al., 2007; Sutton and Soto, 2012; Brewitt and Danner, 2014). However, substantial portions of the Scott River and tributaries lack surface flow during summer, especially in dry years, reducing connectivity between thermal refugia and mainstem habitats.

5.5 Management implications

These models can be used not only to identify the seasonally varying influence of flow, but also to predict future stream temperatures based on managed flow recommendations. Instream flow management frameworks are evolving (Mierau et al., 2017; Poff et al., 2017; Yarnell et al., 2020) and accurate stream temperature models provide a valuable tool for use in those processes. Our modeling approach is relatively easy to implement, especially in comparison to a process-based models, which we hope will facilitate water managers' ability to include stream temperature as a management target. For example, Siskiyou County is currently developing a groundwater sustainability plan for Scott Valley (Foglia et al., 2018). The current groundwater model (Tolley et al., 2019) does not simulate water temperatures, so our temperature model could be a used to assess the effects of groundwater management on groundwater-dependent ecosystems. Our results quantify the effect of flow on stream temperatures, including the CDFW and USFS flow thresholds under consideration and could inform state agencies' development of new flow objectives. The CDFW and USFS flows are both predicted to improve (i.e., cool) summer temperatures relative to current conditions, but improvements would be greater with the higher CDFW flows. We caution that while the CDFW and USFS flows are relatively high compared to observed flows in late summer and early fall, for March to early June they represent extreme drought conditions (Figure 2b), which has two implications. First, in dry years temperatures reach 22 °C in early or mid-June in the observed flow scenario, which is only delayed in a small number of years in the scenarios with CDFW and USFS flows as minimums. Second, if river flows were diverted down to the CDFW and USFS flows in May and June, then the 22 °C threshold would be reached an average of approximately two weeks earlier than occurred with the observed flows (Figure 7c). Surface water diversions for in lieu recharge (switching irrigation source from groundwater to surface water) or managed aquifer recharge (Dahlke et al., 2018; Foglia et al., 2013) should not use the CDFW and USFS flows to guide maximum diversion rates, but instead be tailored to reduce deleterious effects on instream habitat including temperatures, such as ceasing by 1 June, the first date when measured (Figure 2) and modeled temperatures (Figure 7) reach 22 °C.

As with any regression model, prediction accuracy is likely to degrade when applied to conditions more extreme than those present in the calibration dataset. Our calibration dataset includes a wide range of hydrologic conditions, but no years without surface water diversions or groundwater pumping because those activities occur every year. Groundwater modeling efforts suggest that streamflow depletion from groundwater pumping would be greater in dry years than wet years, because in dry years pumping starts earlier, cumulative amounts pumped are greater, and the aquifer is drawn down lower (Foglia et al., 2013; Tolley et al., 2019). Simulated total valley-wide streamflow depletion peaks around 150,000 m^3d^{-1} (60 ft^3/sec) in July and August (Foglia et al., 2013), exceeding streamflow in dry years. Our model should be suitable for modeling stream temperatures in dry years for scenarios with reduced pumping and/or diversions, which would presumably have flows similar to existing wet years (and hence are within the range of calibration flows); however, in wet years such scenarios would likely exceed the range of calibration flows and therefore be subject to considerably higher levels of uncertainty. Any future application of our model to scenarios with flows higher than observed should be done carefully and interpreted with appropriate caveats.

6 Conclusions

Statistical models indicate that river flow has a strong cooling effect on river temperatures during April through July in California's Scott River, similar to previous findings from process-based models in many snow-dominated rivers in western North America. A 24-year dataset of daily streams temperatures allowed us to develop a generalized additive model using tensor product smooths and interactions to represent the non-linear and seasonally varying effects of flow and air temperature on stream temperature. Our model also includes the correlation structures inherent in the data, namely daily temporal autocorrelation and random effects for annual variation. Validation indicated excellent model performance, with average errors ≤1 °C. This project contributes to an emerging body of work demonstrating the benefits of generalized additive models (GAMs) for modeling daily river temperatures. Given the flexibility of GAMs, there is a risk of overfitting data, but this risk can be minimized by restricting the number of knots in GAM smoothers, confirming that smoother shape matches scientific hypotheses regarding the underlying physical processes, and considering whether sample size is adequate for the complexity of the model.

These models identify the specific periods of the year when flow has greatest influence on stream temperatures, and can be used to evaluate the thermal effects of alternative flow management scenarios and prescriptions. The models are implemented in the R software environment with publicly accessible code, and could be applied to model year-round daily temperature in any stream with long-term measurements of flow and water temperature, provided that air temperatures are available from a nearby weather station.

CRediT authorship contribution statement

J. Eli Asarian: Conceptualization, Data curation, Methodology, Formal analysis, Visualization, Writing – original draft, Writing – review & editing. Crystal Robinson: Conceptualization, Investigation, Data curation, Funding acquisition, Project administration, Writing - review & editing.

Acknowledgments

The Klamath Tribal Water Quality Consortium (Karuk Tribe, Yurok Tribe, Hoopa Valley Tribe, Quartz Valley Indian Reservation, and Resighini Rancheria) supported Eli Asarian using funds provided by the U.S. Environmental Protection Agency, Region 9. Maija Meneks (KNF) and Callie McConnell (USFS Corvallis) provided the USFS water temperature data. Isaiah Williams, Alex Case, Sean Ryan and Marla Bennett (QVIR) assisted with data collection. Edward Jones (USGS) provided code for non-linear regression. Laurel Genzoli reviewed a draft of this manuscript.

Data Availability Statement

All data and code are archived in the online repository HydroShare (Asarian and Robinson, 2021, http://www.hydroshare.org/resource/a6653e2919964f9b840ec0340d86e11c). USBR stream temperature data are also available at: https://or.water.usgs.gov/cgi-bin/grapher/graph_setup.pl?basin_id=all&site_id=11519500. Gridded PRISM air temperature data (Daly et al., 2008) are also available at: https://prism.oregonstate.edu/explorer/. GHCN-D air temperature data (Menne et al., 2012a, 2012b) are also available at http://doi.org/10.7289/V5D21VHZ.

References

Amodio, S., Aria, M., & D'Ambrosio, A. (2014). On concurvity in nonlinear and nonparametric regression models. *Statistica*, 74(1), 85–98. https://doi.org/10.6092/issn.1973-2201/4599

Arismendi, I., Safeeq, M., Dunham, J. B., & Johnson, S. L. (2014). Can air temperature be used to project influences of climate change on stream temperature? *Environmental Research Letters*, 9(8), 084015. https://doi.org/10.1088/1748-9326/9/8/084015

Arora, R., Tockner, K., & Venohr, M. (2016). Changing river temperatures in northern Germany: Trends and drivers of change. *Hydrological Processes*, 30(17), 3084–3096. https://doi.org/10.1002/hyp.10849

Asarian, J.E., Cressey, L., Bennett, B., Grunbaum, J., Cyr, L., Soto, T., & Robinson, C. (2020). *Influence of Snowpack, Streamflow, Air Temperature, and Wildfire Smoke on Klamath Basin Stream Temperatures, 1995-2017*. Eureka, CA: Riverbend Sciences. https://doi.org/10.13140/RG.2.2.22934.47681

Asarian, J. E. & Robinson, C. (2021). Data and Codes for: Modeling Seasonal Effects of River Flow on Water Temperatures in an Agriculturally Dominated California River. HydroShare, http://www.hydroshare.org/resource/a6653e2919964f9b840ec0340d86e11c

Asarian, J. E., & Walker, J. D. (2016). Long-Term Trends in Streamflow and Precipitation in Northwest California and Southwest Oregon, 1953-2012. *Journal of the American Water Resources Association*, 52(1), 241–261. https://doi.org/10.1111/1752-1688.12381

Baayen, R. H., van Rij, J., de Cat, C., & Wood, S. (2018). Autocorrelated Errors in Experimental Data in the Language Sciences: Some Solutions Offered by Generalized Additive Mixed Models. In D. Speelman, K. Heylen, & D. Geeraerts (Eds.), *Mixed-Effects Regression Models in Linguistics* (pp. 49–69). Springer International Publishing. https://doi.org/10.1007/978-3-319-69830-4_4

Bartholow, J. M. (1991). A modeling assessment of the thermal regime for an urban sport fishery. *Environmental Management*, 15(6), 833. https://doi.org/10.1007/BF02394821

Benyahya, L., Caissie, D., St-Hilaire, A., Ouarda, T. B. M. J., & Bobée, B. (2007a). A Review of Statistical Water Temperature Models. *Canadian Water Resources Journal / Revue Canadienne Des Ressources Hydriques*, 32(3), 179–192. https://doi.org/10.4296/cwrj3203179

Benyahya, L., St-Hilaire, A., Quarda, T. B. M. J., Bobée, B., & Ahmadi-Nedushan, B. (2007b). Modeling of water temperatures based on stochastic approaches: Case study of the Deschutes River. *Journal of Environmental Engineering and Science*, 6(4), 437–448. https://doi.org/10.1139/s06-067

Benyahya, L., St-Hilaire, A., Ouarda, T., Bobee, B., & Dumas, J. (2008). Comparison of non-parametric and parametric water temperature models on the Nivelle River, France. *Hydrological Sciences Journal*, 53(3), 640–655.

Bernhardt, E. S., Heffernan, J. B., Grimm, N. B., Stanley, E. H., Harvey, J. W., Arroita, M., Appling, A. P., Cohen, M. J., McDowell, W. H., Hall, R. O., Read, J. S., Roberts, B. J., Stets, E. G., & Yackulic, C. B. (2017). The metabolic regimes of flowing waters: Metabolic regimes. *Limnology and Oceanography*. https://doi.org/10.1002/lno.10726

Bodeker, G. E., Boyd, I. S., & Matthews, W. A. (1998). Trends and variability in vertical ozone and temperature profiles measured by ozonesondes at Lauder, New Zealand: 1986–1996. Journal of Geophysical Research: *Atmospheres*, 103(D22), 28661–28681. https://doi.org/10.1029/98JD02581

Boudreault, J., Bergeron, N. E., St-Hilaire, A., & Chebana, F. (2019). Stream temperature modeling using functional regression models. *Journal of the American Water Resources Association*, 55(6), 1382–1400. https://doi.org/10.1111/1752-1688.12778

Boyd, M., and Kasper, B. (2003). Analytical methods for dynamic open channel heat and mass transfer: Methodology for Heat Source model version 7.0. Portland, OR: Oregon Department of Environmental Quality.

Brewitt, K. S., & Danner, E. M. (2014). Spatio-temporal temperature variation influences juvenile steelhead (*Oncorhynchus mykiss*) use of thermal refuges. *Ecosphere*, 5(7), art92. https://doi.org/10.1890/ES14-00036.1

Briggs, M. A., Johnson, Z. C., Snyder, C. D., Hitt, N. P., Kurylyk, B. L., Lautz, L., Irvine, D. J., Hurley, S. T., & Lane, J. W. (2018). Inferring watershed hydraulics and cold-water habitat persistence using multi-year air and stream temperature signals. *Science of The Total Environment*, 636, 1117–1127. https://doi.org/10.1016/j.scitotenv.2018.04.344

Brown, G. W. (1969). Predicting Temperatures of Small Streams. *Water Resources Research*, 5(1), 68–75. https://doi.org/10.1029/WR005i001p00068

Cade, B. S., & Noon, B. R. (2003). A gentle introduction to quantile regression for ecologists. *Frontiers in Ecology and the Environment*, 1(8), 412–420. https://doi.org/10.1890/1540-9295(2003)001[0412:AGITQR]2.0.CO;2

Caissie, D. (2006). The thermal regime of rivers: A review. *Freshwater Biology*, 51(8), 1389–1406. https://doi.org/10.1111/j.1365-2427.2006.01597.x

Caldwell, R. J., Gangopadhyay, S., Bountry, J., Lai, Y., & Elsner, M. M. (2013). Statistical modeling of daily and subdaily stream temperatures: Application to the Methow River Basin, Washington. *Water Resources Research*, 49(7), 4346–4361. https://doi.org/10.1002/wrcr.20353

California Department of Fish and Wildlife (CDFW) (2017). Interim Instream Flow Criteria for the Protection of Fishery Resources in the Scott River Watershed, Siskiyou County. https://web.archive.org/web/20210324204650if_/https://nrm.dfg.ca.gov/FileHandler.ashx?DocumentID=143476.

Chandesris, A., Van Looy, K., Diamond, J. S., & Souchon, Y. (2019). Small dams alter thermal regimes of downstream water. *Hydrology and Earth System Sciences*, 23(11), 4509–4525. https://doi.org/10.5194/hess-23-4509-2019

Cox, N. J. (2006). Speaking Stata: In Praise of Trigonometric Predictors. *The Stata Journal: Promoting Communications on Statistics and Stata*, 6(4), 561–579. https://doi.org/10.1177/1536867X0600600408

Crozier, L. G., Siegel, J. E., Wiesebron, L. E., Trujillo, E. M., Burke, B. J., Sandford, B. P., & Widener, D. L. (2020). Snake River sockeye and Chinook salmon in a changing climate: Implications for upstream migration survival during recent extreme and future climates. *PLOS ONE*, 15(9), e0238886. https://doi.org/10.1371/journal.pone.0238886

Dahlke, H., Brown, A., Orloff, S., Putnam, D., & O'Geen, T. (2018). Managed winter flooding of alfalfa recharges groundwater with minimal crop damage. *California Agriculture*, 72(1), 1–11. https://doi.org/10.3733/ca.2018a0001

Dahlke, F. T., Wohlrab, S., Butzin, M., & Pörtner, H.-O. (2020). Thermal bottlenecks in the life cycle define climate vulnerability of fish. *Science*, 369(6499), 65–70. https://doi.org/10.1126/science.aaz3658

Daly, C., Halbleib, M., Smith, J. I., Gibson, W. P., Doggett, M. K., Taylor, G. H., Curtis, J., & Pasteris, P. P. (2008). Physiographically sensitive mapping of climatological temperature and precipitation across the conterminous United States. *International Journal of Climatology*, 28(15), 2031–2064. https://doi.org/10.1002/joc.1688

David, A. T., Asarian, J. E., & Lake, F. K. (2018). Wildfire Smoke Cools Summer River and Stream Water Temperatures. *Water Resources Research*, 54(10), 7273–7290. https://doi.org/10.1029/2018WR022964

Drake, D., Tate, K., & Carlson, H. (2000). Analysis shows climate-caused decreases in Scott River fall flows. *California Agriculture*, 54(6), 46–49. https://doi.org/10.3733/ca.v054n06p46

Dugdale, S. J., Hannah, D. M., & Malcolm, I. A. (2017). River temperature modelling: A review of process-based approaches and future directions. *Earth-Science Reviews*, 175, 97–113. https://doi.org/10.1016/j.earscirev.2017.10.009

Dugdale, S. J., Malcolm, I. A., Kantola, K., & Hannah, D. M. (2018). Stream temperature under contrasting riparian forest cover: Understanding thermal dynamics and heat exchange processes. *Science of The Total Environment*, 610–611, 1375–1389. https://doi.org/10.1016/j.scitotenv.2017.08.198

Dymond, J. R. (1984). Water temperature change caused by abstraction. *Journal of Hydraulic Engineering*, 110(7), 987–991. https://doi.org/10.1061/(ASCE)0733-9429(1984)110:7(987)

Erickson, T. R., & Stefan, H. G. (2000). Linear Air/Water Temperature Correlations for Streams during Open Water Periods. *Journal of Hydrologic Engineering*, 5(3), 317–321. https://doi.org/10.1061/(ASCE)1084-0699(2000)5:3(317)

Ficklin, D. L., Barnhart, B. L., Knouft, J. H., Stewart, I. T., Maurer, E. P., Letsinger, S. L., & Whittaker, G. W. (2014). Climate change and stream temperature projections in the Columbia River basin: Habitat implications of spatial variation in hydrologic drivers. *Hydrology and Earth System Sciences*, 18(12), 4897–4912. https://doi.org/10.5194/hess-18-4897-2014

FitzGerald, A. M., John, S. N., Apgar, T. M., Mantua, N. J., & Martin, B. T. (2021). Quantifying thermal exposure for migratory riverine species: Phenology of Chinook salmon populations predicts thermal stress. *Global Change Biology*, 27(3), 536–549. https://doi.org/10.1111/gcb.15450

Foglia, L., McNally, A., & Harter, T. (2013). Coupling a spatiotemporally distributed soil water budget with stream-depletion functions to inform stakeholder-driven management of groundwater-dependent ecosystems. *Water Resources Research*, 49(11), 7292–7310. https://doi.org/10.1002/wrcr.20555

Foglia, L., Neumann, J., Tolley, D., Orloff, S., Snyder, R., & Harter, T. (2018). Modeling guides groundwater management in a basin with river–aquifer interactions. *California Agriculture*, 72(1), 84–95. https://doi.org/10.3733/ca.2018a0011

Folegot, S., Hannah, D. M., Dugdale, S. J., Kurz, M. J., Drummond, J. D., Klaar, M. J., Lee-Cullin, J., Keller, T., Martí, E., Zarnetske, J. P., Ward, A. S., & Krause, S. (2018). Low flow controls on stream thermal dynamics. *Limnologica*, 68, 157–167. https://doi.org/10.1016/j.limno.2017.08.003

Fullerton, A. H., Torgersen, C. E., Lawler, J. J., Faux, R. N., Steel, E. A., Beechie, T. J., Ebersole, J. L., & Leibowitz, S. G. (2015). Rethinking the longitudinal stream temperature paradigm: Region-wide comparison of thermal infrared imagery reveals unexpected complexity of river temperatures. *Hydrological Processes*, 29(22), 4719–4737. https://doi.org/10.1002/hyp.10506

Gibeau, P., & Palen, W. J. (2020). Predicted effects of flow diversion by Run-of-River hydropower on bypassed stream temperature and bioenergetics of salmonid fishes. *River Research and Applications*, 36(9), 1903–1915. https://doi.org/10.1002/rra.3706

Gallice, A., Schaefli, B., Lehning, M., Parlange, M. B., & Huwald, H. (2015). Stream temperature prediction in ungauged basins: Review of recent approaches and description of a new physics-derived statistical model. *Hydrol. Earth Syst. Sci.*, 19(9), 3727–3753. https://doi.org/10.5194/hess-19-3727-2015

Gu, R. R., & Li, Y. (2002). River temperature sensitivity to hydraulic and meteorological parameters. *Journal of Environmental Management*, 66(1), 43–56. https://doi.org/10.1006/jema.2002.0565

Gu, R., Montgomery, S., & Austin, T. A. (1998). Quantifying the effects of stream discharge on summer river temperature. *Hydrological Sciences Journal*, 43(6), 885–904. https://doi.org/10.1080/02626669809492185

Hahm, W. J., Rempe, D. M., Dralle, D. N., Dawson, T. E., Lovill, S. M., Bryk, A. B., Bish, D. L., Schieber, J., & Dietrich, W. E. (2019). Lithologically Controlled Subsurface Critical Zone Thickness and Water Storage Capacity Determine Regional Plant Community Composition. *Water Resources Research*, 55(4), 3028–3055. https://doi.org/10.1029/2018WR023760

Helsel, D. R., Hirsch, R. M., Ryberg, K. R., Archfield, S. A., & Gilroy, E. J. (2020). Statistical methods in water resources (*U.S. Geological Survey Techniques and Methods*, book 4, chapter A3). https://doi.org/10.3133/tm4A3

Hilderbrand, R. H., Kashiwagi, M. T., & Prochaska, A. P. (2014). Regional and Local Scale Modeling of Stream Temperatures and Spatio-Temporal Variation in Thermal Sensitivities. *Environmental Management*, 54(1), 14–22. https://doi.org/10.1007/s00267-014-0272-4

Isaak, D. J., Luce, C. H., Horan, D. L., Chandler, G. L., Wollrab, S. P., & Nagel, D. E. (2018). Global Warming of Salmon and Trout Rivers in the Northwestern U.S.: Road to Ruin or Path Through Purgatory? *Transactions of the American Fisheries Society*, 147(3), 566–587. https://doi.org/10.1002/tafs.10059

Isaak, D. J., Wenger, S. J., Peterson, E. E., Hoef, J. M. V., Nagel, D. E., Luce, C. H., Hostetler, S. W., Dunham, J. B., Roper, B. B., Wollrab, S. P., Chandler, G. L., Horan, D. L., & Parkes-Payne, S. (2017). The NorWeST Summer Stream Temperature Model and Scenarios for the Western U.S.: A Crowd-Sourced Database and New Geospatial Tools Foster a User Community and Predict Broad Climate Warming of Rivers and Streams. *Water Resources Research*, 53(11), 9181–9205. https://doi.org/10.1002/2017WR020969

Jackson, F. L., Fryer, R. J., Hannah, D. M., Millar, C. P., & Malcolm, I. A. (2018). A spatio-temporal statistical model of maximum daily river temperatures to inform the management of Scotland's Atlantic salmon rivers under climate change. *Science of The Total Environment*, 612, 1543–1558. https://doi.org/10.1016/j.scitotenv.2017.09.010

Johnson, S. L. (2004). Factors influencing stream temperatures in small streams: Substrate effects and a shading experiment. *Canadian Journal of Fisheries and Aquatic Sciences*, 61(6), 913–923.

Johnson, Z. C., Johnson, B. G., Briggs, M. A., Devine, W. D., Snyder, C. D., Hitt, N. P., Hare, D. K., & Minkova, T. V. (2020). Paired air-water annual temperature patterns reveal hydrogeological controls on stream thermal regimes at watershed to continental scales. *Journal of Hydrology*, 587, 124929. https://doi.org/10.1016/j.jhydrol.2020.124929

Jones, E. C., Perry, R. W., Risley, J. C., Som, N. A., & Hetrick, N. J. (2016). Construction, calibration, and validation of the RBM10 water temperature model for the Trinity River, Northern California (*U.S. Geological Survey Open-File Report* 2016-1056). https://doi.org/10.3133/ofr20161056

Kelleher, C., Wagener, T., Gooseff, M., McGlynn, B., McGuire, K., & Marshall, L. (2012). Investigating controls on the thermal sensitivity of Pennsylvania streams. *Hydrological Processes*, 26(5), 771–785. https://doi.org/10.1002/hyp.8186

Kim, J.-S., & Jain, S. (2010). High-resolution streamflow trend analysis applicable to annual decision calendars: A western United States case study. *Climatic Change*, 102(3–4), 699–707. https://doi.org/10.1007/s10584-010-9933-3

Klamath National Forest (KNF), 2010. Klamath National Forest Sediment and Temperature Monitoring Plan and Quality Assurance Project Plan. Yreka, CA: Klamath National Forest. https://web.archive.org/web/http://www.waterboards.ca.gov/water_issues/programs/tmdl/records/region_1/2013/ref4082.pdf.

Koch, H., & Grünewald, U. (2010). Regression models for daily stream temperature simulation: Case studies for the river Elbe, Germany. *Hydrological Processes*, 24(26), 3826–3836. https://doi.org/10.1002/hyp.7814

Kothandaraman, V. (1971). Analysis of Water Temperature Variations in Large River. *Journal of the Sanitary Engineering Division*, 97(1), 19–31. https://doi.org/10.1061/JSEDAI.0001242

Laanaya, F., St-Hilaire, A., & Gloaguen, E. (2017). Water temperature modelling: Comparison between the generalized additive model, logistic, residuals regression and linear regression models. *Hydrological Sciences Journal*, 62(7), 1078–1093. https://doi.org/10.1080/02626667.2016.1246799

Leach, J. A., & Moore, R. D. (2019). Empirical stream thermal sensitivities may underestimate stream temperature response to climate warming. *Water Resources Research*, 55(7), 5453–5467. https://doi.org/10.1029/2018WR024236

Lee, S.-Y., Fullerton, A. H., Sun, N., & Torgersen, C. E. (2020). Projecting spatiotemporally explicit effects of climate change on stream temperature: A model comparison and implications for coldwater fishes. *Journal of Hydrology*, 588, 125066. https://doi.org/10.1016/j.jhydrol.2020.125066

Letcher, B. H., Hocking, D. J., O'Neil, K., Whiteley, A. R., Nislow, K. H., & O'Donnell, M. J. (2016). A hierarchical model of daily stream temperature using air-water temperature synchronization, autocorrelation, and time lags. PeerJ, 4, e1727. https://doi.org/10.7717/peerj.1727

Li, H., Deng, X., Kim, D.-Y., & Smith, E. P. (2014). Modeling maximum daily temperature using a varying coefficient regression model. *Water Resources Research*, 50(4), 3073–3087. https://doi.org/10.1002/2013WR014243

Liu, S., Xie, Z., Liu, B., Wang, Y., Gao, J., Zeng, Y., Xie, J., Xie, Z., Jia, B., Qin, P., Li, R., Wang, L., & Chen, S. (2020). Global river water warming due to climate change and anthropogenic heat emission. *Global and Planetary Change*, 193, 103289. https://doi.org/10.1016/j.gloplacha.2020.103289

Luce, C., Staab, B., Kramer, M., Wenger, S., Isaak, D., & McConnell, C. (2014). Sensitivity of summer stream temperatures to climate variability in the Pacific Northwest. *Water Resources Research*, 50(4), 3428–3443. https://doi.org/10.1002/2013WR014329

Luo, Y., Ficklin, D. L., Liu, X., & Zhang, M. (2013). Assessment of climate change impacts on hydrology and water quality with a watershed modeling approach. Science of The Total Environment, 450–451, 72–82. https://doi.org/10.1016/j.scitotenv.2013.02.004

Lusardi, R. A., Hammock, B. G., Jeffres, C. A., Dahlgren, R. A., & Kiernan, J. D. (2019). Oversummer growth and survival of juvenile coho salmon (Oncorhynchus kisutch) across a natural gradient of stream water temperature and prey availability: An in situ enclosure experiment. Canadian Journal of Fisheries and Aquatic Sciences, 1–12. https://doi.org/10.1139/cjfas-2018-0484

Manhard, C. V., N. A. Som, E. C. Jones, & R. W. Perry. 2018. Estimation of stream conditions in tributaries of the Klamath River, Northern California (*Arcata Fisheries Technical Report* Number TR 2018-32). Arcata, CA: U.S. Fish and Wildlife Service. https://web.archive.org/web/https://www.fws.gov/arcata/fisheries/reports/technical/2018/EstimationofStreamConditionsinTributariesoftheKlamathRiverNorthernCalifornia.pdf

Mayer, T. D. (2012). Controls of summer stream temperature in the Pacific Northwest. *Journal of Hydrology*, 475(0), 323–335. https://doi.org/10.1016/j.jhydrol.2012.10.012

McGrath, E. O., Neumann, N. N., & Nichol, C. F. (2017). A Statistical Model for Managing Water Temperature in Streams with Anthropogenic Influences. *River Research and Applications*, 33(1), 123–134. https://doi.org/10.1002/rra.3057

Meier, W., Bonjour, C., Wüest, A., & Reichert, P. (2003). Modeling the Effect of Water Diversion on the Temperature of Mountain Streams. Journal of Environmental Engineering, 129(8), 755–764. https://doi.org/10.1061/(ASCE)0733-9372(2003)129:8(755)

Menne, M.J., Durre, I., Korzeniewski, B., McNeal, S., Thomas, K., Yin, X., Anthony, S., Ray, R., Vose, R.S., Gleason, B.E., & Houston, T.G. (2012a). Global Historical Climatology Network - Daily (GHCN-Daily), Version 3.26. NOAA National Climatic Data Center. http://doi.org/10.7289/V5D21VHZ. Accessed 2021-01-11

Menne, M. J., Durre, I., Vose, R. S., Gleason, B. E., & Houston, T. G. (2012b). An Overview of the Global Historical Climatology Network-Daily Database. Journal of Atmospheric and Oceanic Technology, 29(7), 897–910. https://doi.org/10.1175/JTECH-D-11-00103.1

Mierau, D. W., Trush, W. J., Rossi, G. J., Carah, J. K., Clifford, M. O., & Howard, J. K. (2017). Managing diversions in unregulated streams using a modified percent-of-flow approach. Freshwater Biology. https://doi.org/10.1111/fwb.12985

Mohseni, O., Stefan, H. G., & Erickson, T. R. (1998). A nonlinear regression model for weekly stream temperatures. *Water Resources Research*, 34(10), 2685–2692. https://doi.org/10.1029/98WR01877

Moore, D. R., Spittlehouse, D. L., & Story, A. (2005a). Riparian Microclimate and Stream Temperature Response to Forest Harvesting: A Review. *Journal of the American Water Resources Association*, 41(4), 813–834. https://doi.org/10.1111/j.1752-1688.2005.tb03772.x

Moore, R. D., Sutherland, P., Gomi, T., & Dhakal, A. (2005b). Thermal regime of a headwater stream within a clear-cut, coastal British Columbia, Canada. *Hydrological Processes*, 19(13), 2591–2608. https://doi.org/10.1002/hyp.5733

Moulton, T. L. (2018). *rMR: Importing Data from Loligo Systems Software, Calculating Metabolic Rates and Critical Tensions*. R package version 1.1.0. https://CRAN.R-project.org/package=rMR

Muggeo, V. M. R., Sciandra, M., Tomasello, A., & Calvo, S. (2013). Estimating growth charts via nonparametric quantile regression: A practical framework with application in ecology. *Environmental and Ecological Statistics*, 20(4), 519–531. https://doi.org/10.1007/s10651-012-0232-1

National Marine Fisheries Service (NMFS) (2014). Final Recovery Plan for the Southern Oregon/Northern California Coast Evolutionarily Significant Unit of Coho Salmon (*Oncorhynchus kisutch*). Arcata, CA: National Marine Fisheries Service.

Neumann David W., Rajagopalan Balaji, & Zagona Edith A. (2003). Regression Model for Daily Maximum Stream Temperature. Journal of Environmental Engineering, 129(7), 667–674. https://doi.org/10.1061/(ASCE)0733-9372(2003)129:7(667)

Nichols, A. L., Willis, A. D., Jeffres, C. A., & Deas, M. L. (2014). Water temperature patterns below large groundwater springs: management implications for coho salmon in the Shasta River, California. *River Research and Applications*, 30(4), 442–455. https://doi.org/10.1002/rra.2655

North Coast Regional Water Quality Control Board (NCRWQCB) (2005). *Staff Report for the Action Plan for the Scott River Watershed Sediment and Temperature Total Maximum Daily*

Loads. Santa Rosa, CA: North Coast Regional Water Quality Control Board. https://www.waterboards.ca.gov/northcoast/water_issues/programs/tmdls/scott_river/staff_report

Null, S. E., Mouzon, N. R., & Elmore, L. R. (2017). Dissolved oxygen, stream temperature, and fish habitat response to environmental water purchases. *Journal of Environmental Management*, 197, 559–570. https://doi.org/10.1016/j.jenvman.2017.04.016

Null, S. E., Viers, J. H., Deas, M. L., Tanaka, S. K., & Mount, J. F. (2013). Stream temperature sensitivity to climate warming in California's Sierra Nevada: Impacts to coldwater habitat. *Climatic Change*, 116(1), 149–170. https://doi.org/10.1007/s10584-012-0459-8

Ouellet, V., St-Hilaire, A., Dugdale, S. J., Hannah, D. M., Krause, S., & Proulx-Ouellet, S. (2020). River temperature research and practice: Recent challenges and emerging opportunities for managing thermal habitat conditions in stream ecosystems. *Science of The Total Environment*, 736, 139679. https://doi.org/10.1016/j.scitotenv.2020.139679

Pedersen, E. J., Miller, D. L., Simpson, G. L., & Ross, N. (2019). Hierarchical generalized additive models in ecology: An introduction with mgcv. *PeerJ*, 7, e6876. https://doi.org/10.7717/peerj.6876

Persad, G. G., Swain, D. L., Kouba, C., & Ortiz-Partida, J. P. (2020). Inter-model agreement on projected shifts in California hydroclimate characteristics critical to water management. *Climatic Change*. https://doi.org/10.1007/s10584-020-02882-4

Pinheiro, J., Bates, D., DebRoy, S., Sarkar, D.., & R Core Team (2020). *nlme: Linear and Nonlinear Mixed Effects Models*. R package version 3.1-148. https://CRAN.R-project.org/package=nlme.

Piotrowski, A. P., & Napiorkowski, J. J. (2019). Simple modifications of the nonlinear regression stream temperature model for daily data. *Journal of Hydrology*, 572, 308–328. https://doi.org/10.1016/j.jhydrol.2019.02.035

Poff, N. L., Tharme, R. E., & Arthington, A. H. (2017). Chapter 11—Evolution of Environmental Flows Assessment Science, Principles, and Methodologies. In A. C. Horne, J. A. Webb, M. J. Stewardson, B. Richter, & M. Acreman (Eds.), *Water for the Environment* (pp. 203–236). Academic Press. https://doi.org/10.1016/B978-0-12-803907-6.00011-5

Power, M. E., & Dietrich, W. E. (2002). Food webs in river networks. *Ecological Research*, 17(4), 451–471.

Quartz Valley Indian Reservation (QVIR) (2016). *Quality Assurance Project Plan 2016 Revision Water Quality Sampling and Analysis, CWA 106 grant identification # I-96927206-0*. Fort Jones, CA: QVIR Tribal Environmental Protection Department.

Quigley, D., Färber, S., Conner, K., Power, J., & Bundy, L. (2001). Water Temperatures in the Scott River Watershed in Northern California. https://web.archive.org/web/http://www.fws.gov/yreka/Final-Reports/rmaap/2000-JITW-01-SRCD.pdf

R Core Team (2020). *R: A language and environment for statistical computing*. Vienna, Austria: R Foundation for Statistical Computing. https://www.R-project.org/.

Rahmani, F., Lawson, K., Ouyang, W., Appling, A., Oliver, S., & Shen, C. (2020). Exploring the exceptional performance of a deep learning stream temperature model and the value of streamflow data. Environmental Research Letters. https://doi.org/10.1088/1748-9326/abd501

Santiago, J. M., Muñoz-Mas, R., Solana-Gutiérrez, J., García de Jalón, D., Alonso, C., Martínez-Capel, F., Pórtoles, J., Monjo, R., & Ribalaygua, J. (2017). Waning habitats due to climate change: The effects of changes in streamflow and temperature at the rear edge of the distribution of a cold-water fish. *Hydrology and Earth System Sciences*, 21(8), 4073–4101. https://doi.org/10.5194/hess-21-4073-2017

Segura, C., Caldwell, P., Sun, G., McNulty, S., & Zhang, Y. (2015). A model to predict stream water temperature across the conterminous USA. *Hydrological Processes*, 29(9), 2178–2195. https://doi.org/10.1002/hyp.10357

Siegel, J. E., & Volk, C. J. (2019). Accurate spatiotemporal predictions of daily stream temperature from statistical models accounting for interactions between climate and landscape. *PeerJ*, 7, e7892. https://doi.org/10.7717/peerj.7892

Sinokrot, B. A., & Gulliver, J. S. (2000). In-stream flow impact on river water temperatures. *Journal of Hydraulic Research*, 38(5), 339–349. https://doi.org/10.1080/00221680009498315

Sohrabi, M. M., Benjankar, R., Tonina, D., Wenger, S. J., & Isaak, D. J. (2017). Estimation of daily stream water temperatures with a Bayesian regression approach. *Hydrological Processes*, 31(9), 1719–1733. https://doi.org/10.1002/hyp.11139

Soto, B. (2016). Assessment of Trends in Stream Temperatures in the North of the Iberian Peninsula Using a Nonlinear Regression Model for the Period 1950–2013. *River Research and Applications*, 32(6), 1355–1364. https://doi.org/10.1002/rra.2971

Stanford, J.A. & Ward, J.V. (1992). Management of Aquatic Resources in Large Catchments: Recognizing Interactions Between Ecosystem Connectivity and Environmental Disturbance. In R. J. Naiman (Editor). *Watershed Management: Balancing Sustainability and Environmental Change* (pp. 91–124). New York, NY: Springer.

St-Hilaire, A., Boyer, C., Bergeron, N., & Daigle, A. (2018). Water temperature monitoring in Eastern Canada: A case study for network optimization. *WIT Transactions on Ecology and the Environment*, 228, 269–275. https://doi.org/10.2495/WP180251

Steel, E. A., Kennedy, M. C., Cunningham, P. G., & Stanovick, J. S. (2013). Applied statistics in ecology: Common pitfalls and simple solutions. *Ecosphere*, 4(9), art115. https://doi.org/10.1890/ES13-00160.1

Steel, E. A., Tillotson, A., Larsen, D. A., Fullerton, A. H., Denton, K. P., & Beckman, B. R. (2012). Beyond the mean: The role of variability in predicting ecological effects of stream temperature on salmon. *Ecosphere*, 3(11), 1–11. https://doi.org/10.1890/ES12-00255.1

Stenhouse, S., Pisano, M., Bean, C., & Chesney, W. (2012). Water temperature thresholds for coho salmon in a spring fed river, Siskiyou County, California. *California Fish and Game*, 98(1), 19–37.

Superior Court of Siskiyou County (1980). Scott River Adjudication, Decree No. 30662. Scott River Stream System, Siskiyou County. Sacramento, CA: State Water Resources Control Board.

Sutton, R. J., Deas, M. L., Tanaka, S. K., Soto, T., & Corum, R. A. (2007). Salmonid observations at a Klamath River thermal refuge under various hydrological and meteorological conditions. *River Research and Applications*, 23(7), 775–785.

Sutton, R., & Soto, T. (2012). Juvenile coho salmon behavioural characteristics in Klamath river summer thermal refugia. *River Research and Applications*. https://doi.org/10.1002/rra.1459

Tan, J., & Cherkauer, K. A. (2013). Assessing stream temperature variation in the Pacific Northwest using airborne thermal infrared remote sensing. *Journal of Environmental Management*, 115, 206–216. https://doi.org/10.1016/j.jenvman.2012.10.012

Toffolon, M., & Piccolroaz, S. (2015). A hybrid model for river water temperature as a function of air temperature and discharge. *Environmental Research Letters*, 10(11), 114011. https://doi.org/10.1088/1748-9326/10/11/114011

Tolley, D., Foglia, L., & Harter, T. (2019). Sensitivity Analysis and Calibration of an Integrated Hydrologic Model in an Irrigated Agricultural Basin With a Groundwater-Dependent Ecosystem. *Water Resources Research*, 55(9), 7876–7901. https://doi.org/10.1029/2018WR024209

Van Kirk, R. W., & Naman, S. W. (2008). Relative Effects of Climate and Water Use on Base-Flow Trends in the Lower Klamath Basin. *Journal of the American Water Resources Association*, 44(4), 1035–1052. https://doi.org/10.1111/j.1752-1688.2008.00212.x

van Rij, J., Hendriks, P., van Rijn, H., Baayen, R. H., & Wood, S. N. (2019). Analyzing the Time Course of Pupillometric Data. *Trends in Hearing*, 23, 233121651983248. https://doi.org/10.1177/2331216519832483

van Rij, J., Wieling, M., Baayen, R., van Rijn, H. (2020). *itsadug: Interpreting Time Series and Autocorrelated Data Using GAMMs*. R package version 2.4. https://cran.r-project.org/package=itsadug

van Vliet, M. T. H., Ludwig, F., Zwolsman, J. J. G., Weedon, G. P., & Kabat, P. (2011). Global river temperatures and sensitivity to atmospheric warming and changes in river flow. *Water Resources Research*, 47(2). https://doi.org/10.1029/2010WR009198

Wanders, N., Vliet, M. T. H. van, Wada, Y., Bierkens, M. F. P., & Beek, L. P. H. (Rens) van. (2019). High-Resolution Global Water Temperature Modeling. *Water Resources Research*, 55(4), 2760–2778. https://doi.org/10.1029/2018WR023250

Webb, B. W., Clack, P. D., & Walling, D. E. (2003). Water–air temperature relationships in a Devon river system and the role of flow. *Hydrological Processes*, 17(15), 3069–3084. https://doi.org/10.1002/hyp.1280

Webb, B. W., Hannah, D. M., Moore, R. D., Brown, L. E., & Nobilis, F. (2008). Recent advances in stream and river temperature research. *Hydrological Processes*, 22(7), 902–918. https://doi.org/10.1002/hyp.6994

Webb, B. W., & Walling, D. E. (1993). Temporal variability in the impact of river regulation on thermal regime and some biological implications. *Freshwater Biology*, 29(1), 167–182. https://doi.org/10.1111/j.1365-2427.1993.tb00752.x

Welsh, H. H., Hodgson, G. R., Harvey, B. C., & Roche, M. F. (2001). Distribution of Juvenile Coho Salmon in Relation to Water Temperatures in Tributaries of the Mattole River, California.

North American Journal of Fisheries Management, 21(3), 464–470. https://doi.org/10.1577/1548-8675(2001)021<0464:DOJCSI>2.0.CO;2

Wenger, S. J., Isaak, D. J., Luce, C. H., Neville, H. M., Fausch, K. D., Dunham, J. B., Dauwalter, D. C., Young, M. K., Elsner, M. M., Rieman, B. E., Hamlet, A. F., & Williams, J. E. (2011). Flow regime, temperature, and biotic interactions drive differential declines of trout species under climate change. *Proceedings of the National Academy of Sciences*, 108(34), 14175–14180. https://doi.org/10.1073/pnas.1103097108

Wondzell, S. M., Diabat, M., & Haggerty, R. (2019). What Matters Most: Are Future Stream Temperatures More Sensitive to Changing Air Temperatures, Discharge, or Riparian Vegetation? *Journal of the American Water Resources Association*, 55(1), 116–132. https://doi.org/10.1111/1752-1688.12707

Wood, S.N. (2017). *Generalized Additive Models: An Introduction with R (2nd edition)*. Chapman and Hall/CRC.

Yang, G., & Moyer, D. L. (2020). Estimation of nonlinear water-quality trends in high-frequency monitoring data. *Science of The Total Environment*, 715, 136686. https://doi.org/10.1016/j.scitotenv.2020.136686

Yard, M. D., Bennett, G. E., Mietz, S. N., Coggins, L. G., Stevens, L. E., Hueftle, S., & Blinn, D. W. (2005). Influence of topographic complexity on solar insolation estimates for the Colorado River, Grand Canyon, AZ. *Ecological Modelling*, 183(2), 157–172. https://doi.org/10.1016/j.ecolmodel.2004.07.027

Yarnell, S. M., Stein, E. D., Webb, J. A., Grantham, T., Lusardi, R. A., Zimmerman, J., Peek, R. A., Lane, B. A., Howard, J., & Sandoval-Solis, S. (2020). A functional flows approach to selecting ecologically relevant flow metrics for environmental flow applications. River Research and Applications, rra.3575. https://doi.org/10.1002/rra.3575

Zhu, S., Heddam, S., Nyarko, E. K., Hadzima-Nyarko, M., Piccolroaz, S., & Wu, S. (2018). Modeling daily water temperature for rivers: Comparison between adaptive neuro-fuzzy inference systems and artificial neural networks models. *Environmental Science and Pollution Research*. https://doi.org/10.1007/s11356-018-3650-2

Zhu, S., & Piotrowski, A. P. (2020). River/stream water temperature forecasting using artificial intelligence models: A systematic review. *Acta Geophysica*, 68(5), 1433–1442. https://doi.org/10.1007/s11600-020-00480-7

Zillig, K. W., Lusardi, R. A., Moyle, P. B., & Fangue, N. A. (2021). One size does not fit all: Variation in thermal eco-physiology among Pacific salmonids. *Reviews in Fish Biology and Fisheries*. https://doi.org/10.1007/s11160-020-09632-w